coatings

MDPI

Article

The Use of Polyurethane Composites with Sensing Polymers as New Coating Materials for Surface Acoustic Wave-Based Chemical Sensors—Part II: Polyurethane Composites with Polylaurylmetacrylate, Polyisobutene, and Poly(chlorotrifluoroethylene-co-vinylidene Fluoride): Coating Results, Relative Sensor Responses and Adhesion Analysis

Mauro dos Santos de Carvalho [1,*], Michael Rapp [2,*], Achim Voigt [2] and Marian Dirschka [2]

[1] Instituto de Química, Universidade Federal do Rio de Janeiro, Avenida Athos da Silveira Ramos, 149 Bloco A, 4º Andar, SALA 408 Cidade Universitária, Rio de Janeiro CEP, Rio de Janeiro 21941-909, Brazil
[2] Institute of Microstructure Technology, Karlsruhe Institute of Technology, Hermann-von-Helmholtz-Platz 1, 76344 Eggenstein-Leopoldshafen, Germany
* Correspondence: mauro@iq.ufrj.br (M.d.S.d.C.); michael.rapp@partner.kit.edu (M.R.)

Abstract: This work presents the application of the methodology for the sensitization of surface acoustic wave-based sensors (SAW), developed in the first part of this work. The strategy of the method is the obtention of sensing layers with tailored chemical environments by taking advantage of the wide variety of chemical composition of the organic polymers, which have been used as sensing polymers, and combining them with polyurethane (PU) to form polymeric composites that show enhanced properties as sensing materials for the SAW sensor technology. In the first part of this work, the ultrasonic and adhesion characterization was correlated to the sensor responses of PU-polybutylmethacrylate (PBMA) composites of different relative concentrations of the sensing polymer (PBMA) and PU. The resulting coating layers obtained with the PU polymer composites improved the chemical and mechanical properties of the sensing layer without interfering with the quality of their sensor responses in comparison to those with the pristine polymer as the sensing material. In this second part of this work, three new polyurethane polymeric composites were analyzed. The new sensing materials were produced using polylaurylmetacrylate (PLMA), polyisobutene (PIB), and poly(chlorotrifluoroethylene-co-vinylidene fluoride) (PCTFE) as the sensing polymers combined with PU. The results of the new PU polymer composites showed consequently different properties depending on the type of sensing polymer used, reproducing, however, the previous features achieved with PU and polybutylmetacrylate (PBMA) composites, like the improvements in the adhesion and the resistance against an organic solvent and preserving, in each case, the sensor response characteristic of each sensing polymer used, as was also observed for the PU-PBMA polymeric composites. The results obtained with the new sensing materials validated the strategy and confirmed its generalization as a very suitable methodology for the sensitization of SAW sensors, strongly indicating the applicability and reliability of the method, which makes possible the choice of virtually any chemical environments for the sensitization of SAW sensor systems.

Keywords: polymeric sensing layer; chemical sensitization; coating analysis

Citation: Carvalho, M.d.S.d.; Rapp, M.; Voigt, A.; Dirschka, M. The Use of Polyurethane Composites with Sensing Polymers as New Coating Materials for Surface Acoustic Wave-Based Chemical Sensors—Part II: Polyurethane Composites with Polylaurylmetacrylate, Polyisobutene, and Poly(chlorotrifluoroethylene-co-vinylidene Fluoride): Coating Results, Relative Sensor Responses and Adhesion Analysis. *Coatings* **2024**, *14*, 778. https://doi.org/10.3390/coatings14070778

Academic Editor: Arūnas Ramanavičius

Received: 12 April 2024
Revised: 7 June 2024
Accepted: 13 June 2024
Published: 21 June 2024

1. Introduction

SAW sensors have been largely employed in chemical and gas sensing due to their sensitivity, precision, fast responses, and affordable cost. This includes the detection of chemical warfare agents, explosives, organic and inorganic vapors, and environmental monitoring to detect diseases, just to mention a few from the wide range of the gas sensing

applications of the SAW sensors [1–5]. The SAW technology for gas sensing has been continuously improving, mostly through the development of many new sensing materials that have enhanced the properties of the SAW sensors [6].

The SAW sensor element usually consists of a piezoelectric substrate where contact and interdigitated electrodes are patterned over the surface. The design and structure of the IDT used in this work were optimized to enhance the sensor responses [7]. The electrical circuit provides the mechanical energy through the electrodes to create the acoustic waves that propagate on the surface of the piezoelectric substrate and are monitored by the circuit. By the operation of the SAW sensor system, changes on the surface of the substrate on the molecular level by the interaction with the analytes can be detected as frequency and attenuation changes through ultrasonic measurements. The resulting mass loading effect, which changes the acoustic velocity and, subsequently, affects the frequency shift, is utilized for sensing purposes [8,9]. The surface of the SAW sensor element should, therefore, be sensitized by the deposition of a suitable coating layer to create, ideally, the appropriate chemical environment for the interaction with the target analytes. Through this mechanism, SAW sensors can sense interactions on the surface with a very high sensitivity [10,11].

The development of the SAW sensor systems continues, mostly to improve and discover new sensing materials and the coating process. Once the electronics and the hardware of the system have been adequately developed to support most of the applications, they will be eventually subject to a design enhancement of the sensor array or the necessary actualization of the electronic component technology [12,13].

The main goal of the development of new sensing materials for SAW technology is the enhancement of the selectivity of the sensors that, together with the characteristic high sensitivity of the SAW methodology, can expand the specificity and the limits of the detection method, as in the case of trace analytes in complex matrices [14]. The chemical and mechanical properties of the sensing materials play a decisive role in the performance enhancement of the SAW sensors. The achievement of selective and precise sensor responses demands not only an optimized chemical sensing environment but also a high uniformity of the resulting structure of the sensitized coating layer together with a high homogeneity of the material distribution obtained by the coating process. Both factors will account for minimizing the attenuation of the wave propagation throughout the coated surface and advancing the sorption capacity of the sensing layer. In addition to those features of the coated sensitized materials, a reliable reproducibility of the sensor sensitization process, together with the necessary mechanical and chemical stability to ensure adequate long-term sensor application, is also mandatory to enable the utilization of the sensor system in real applications [15].

Among the wide range of sensing materials used in the SAW sensor technology for gas sensing applications, organic polymers have been one of the most used due to their advantages, like cost and availability [16]. The large variety of chemical compositions available by the equally large diversity of polymers offers a large and affordable spectrum of chemical environments. Additionally, in practice, most organic polymers can be easily deposited over the surface of the piezoelectric substrates by most of the coating methods used, like spray coating, spin coating, and matrix-assisted pulsed laser evaporation [17–20].

The initial use of pristine polymers as coating sensing materials gave rise to issues of adhesion to the surface of the piezoelectric substrate elements, and dewetting of the polymeric coating was observed, most probably due to the lack of chemical compatibility between some polymers and the surface of the sensor substrates [21–24].

After the initial use of pristine polymers as the sole sensing materials, many studies have been conducted looking to explore other properties of polymers than just their function as the chemical environment for the sensitization, providing different ways of support in composites with diverse types of materials, enhancing their properties, and giving rise to new types of composite sensing materials for the SAW technology [25–30].

Different types of polymer composites have been presented as new classes of sensing materials, in which the polymers are combined with various substances and materials,

ranging from particles of chemical compounds, graphene, carbon nanotubes to quantum dots, to mention just a few of them [26,28,31–33]. The organic polymer present in the composites does not act as the chemical transducer itself but provides different support functions to the sensing process. Among the polymers that have a support function in chemical sensor technologies, polyurethanes play a coadjutant role in the transduction of many types of sensors, enhancing sensing properties of the methods, ranging from chemiresistive, colorimetric, pressure, and temperature to conductimetric and humidity sensors [34–43].

In this context, we devised a methodology for the development of a new type of coating materials for the SAW technology that can take advantage of the large possibilities of the chemical sensing environment presented by the organic polymers as coating materials, combined with the structuring features of the polyurethanes. These new coating materials can be deposited by the spin coating method with high reproducibility, and the obtained coating fulfills all the requirements of a sensing layer, yet greatly improving the sensing possibilities for the SAW sensor technology by tailoring the chemical environment of the coating layer and, thus, improving the sensor selectivity for any desired analyte.

New developed sensing materials are composed of polyurethane and, at least, a second polymer that acts as the sensing polymer. In the first part of this work, we present the results of the methodology for the polymer composites formed by PBMA as the sensing polymer and polyurethane and their overall practical evaluation as sensing layers for their application in the SAW technology [44]. The results for the composites of PU with PBMA showed that the methodology generated reliable sensor coatings, with improved adhesion and chemical resistance regarding the test of immersion in an organic solvent (perchloroethylene), maintaining the sensitivity characteristics of the sensing polymer (PBMA) and fulfilling all the other requirements to be used in the SAW sensor device [44].

The results for the PU-PBMA composites suggested that the presence of PU in the composites accounts for improved adhesion to the surface of the sensor element, providing, at the same time, a structure to the composite that can withstand the chemical resistance and adhesion test (CAT). It was also inferred that, depending on the relative concentration of PBMA and PU in the composite, some excess of the sensing polymer (PBMA) remained as not nonbound in the PU-PBMA structure of the coating layer. According to the results, this excess should be removed from the composite coating layers during the CAT [44].

In the second part of this work, the methodology was applied to other three new PU polymer composites obtained with three other sensing polymers with distinct chemical constitutions—polylaurylmetacrylate (PLMA), polyisobutene (PIB), and poly(chlorotrifluoroethylene-co-vinylidene fluoride) (PCTFE)—as a proof of concept and for the generalization of the developed sensor sensing methodology. The results of the coating process in terms of the behavior regarding the properties of coating layers for SAW sensors, adhesion to the sensor surface of these new PU polymer composites, and sensor responses to chemically different analytes were evaluated.

2. Methodology

2.1. SAW Sensor System and Piezoelectric Quartz Sensor Elements

The quartz sensor elements are highly polished piezoelectric quartz (SiO_2, 37.5° cut orientation, 0.5 mm thickness) devices with gold electrodes lithographically deposited, with an optimized geometry [7], purchased from SCD Components, Dresden, Germany. The SAW sensor system was developed internally and is described in the first part of the work [44].

2.2. Chemicals

Chloroform (CAS 67-66-3), perchloroethylene (CAS 127-18-4), toluene (CAS 108-88-3), and p-xylene (CAS 106-42-3) were purchased from Sigma-Aldrich Co. (St. Louis, MO, USA), all having concentrations higher than 99%, and were used without further treatment. Polylaurylmetacrylate (CAS 25719-52-2), polyisobutylene (CAS 9003-27-4), and

poly(chlorotrifluoroethylene-co-vinylidene fluoride) (CAS 9010-75-7) were purchased from Sigma-Aldrich Co., (St. Louis, MO, USA).

2.3. Coating Procedure

The deposition of the coating materials was made by dispensing 200 microliters of the spin coating solutions (Tables 1–3) using a micropipette over the sensor element placed at the spin coater (Laurell MS-400B-6NPP/LITE,, Lansdale, PA, USA). The spin coater was immediately turned on at a rotation speed of 8000 rpm for 120 s for all experiments. All parameters were precisely controlled.

Table 1. Composition of the spin coating solutions for the PU-PLMA composites.

Description	PLMA/mg.100 mL^{-1}	PU/mg.100 mL^{-1}
PLMA_200	0.8	0.0
PU_50	0.0	0.8
PLMA_100+PU_50	0.4	0.8
PLMA_200+PU_50	0.8	0.8
PLMA_300+PU_50	1.2	0.8
PLMA_400+PU_50	1.6	0.8

Table 2. Composition of the spin coating solutions for the PU-PIB composites.

Description	PIB/mg.100 mL^{-1}	PU/mg.100 mL^{-1}
PIB_200	0.4	0.0
PU_50	0.0	0.8
PIB_100+PU_50	0.2	0.8
PIB_200+PU_50	0.4	0.8
PIB_300+PU_50	0.6	0.8
PIB_400+PU_50	0.8	0.8

Table 3. Composition of the spin coating solutions for the PU-PCTFE composites.

Description	PCTFE/mg.100 mL^{-1}	PU/mg.100 mL^{-1}
PCTFE_200	0.8	0.0
PU_50	0.0	0.8
PCTFE_100+PU_50	0.4	0.8
PCTFE_200+PU_50	0.8	0.8
PCTFE_300+PU_50	1.2	0.8
PCTFE_400+PU_50	1.6	0.8

2.4. Ultrasonic Measurements

The ultrasonic parameters, frequency shift and acoustic attenuation (S_{21} parameter), were recorded using a HF-Network Analyzer (Hewlett Packard 8712ES, Waldbronn, Germany). The attenuation and phase transmission plots were compared with the corresponding necessary parameters required for stable operation in the electrical RF oscillators.

2.5. Relative Sensor Responses with Saturated Vapors of the Analytes

The procedure and the experimental setup for the measurements of the sensor responses are described in the first part of this work [44]. The sensor responses for each coating material were obtained by measuring the maximum frequency shift with the SAW

sensor system for the same nine organic compounds and water as in the previous work. The relative sensor responses were calculated by taking the signal of the sensor coated with the pristine sensing polymer as the reference, without (purging) and with analyte sampling conditions. The results for chloroform and p-xylene as the analytes are exemplarily presented in this work. The results for the other eight organic analytes and water will be discussed in the frame of the sensor selectivity in our future work.

2.6. Chemical Resistance and Adhesion Test (CAT)

The CAT test is a house-made test devised to investigate the stability of the polymeric coating layer in terms of its chemical resistance to perchloroethylene, a strong organic solvent, and, at the same time, to infer the adhesion of the polymeric layer to the sensor element surface. The method, described in the first part of this work [44], is performed by submitting the coated sensor elements to the limit condition of a complete immersion in a bath of perchloroethylene for 24 h. After this, the coated sensor is left at room temperature for twelve hours to complete the evaporation of the solvent before the measurements.

2.7. Sensor Responses Due to the Coating Itself

The sensor responses are strongly affected by the coating itself. There are two main reasons for this: the uniformity of the coating, which results in scattering of the surface acoustic wavefronts (toward non-parallelism), and the viscoelastic properties (or intrinsic damping) introduced by the polymer layer material itself. In general, the attenuation of the SAW device is increased by both effects compared with the uncoated state. If the attenuation of a SAW device is increased, the Q-factor, of course, will be lowered as well.

2.8. Production of the Coated SAW

The SAW sensors were coated with the pure polymers (PLMA, PIB, PCTFE, and PU) and with the corresponding PU composites, whose compositions are presented in Tables 1–3, for the combination with PLMA, PIB, and PCTFE, respectively, using the coating procedure described in Section 2.3. The concentrations of the polymers in each case were determined by their solubility in solvents, to achieve the operational parameters needed for their proper work in the sensor system to obtain their respective sensor responses.

3. Results and Discussion

3.1. Analysis of the Coating Process: Ultrasonic Parameters

The analysis of the coating performance is conducted by the interpretation of the ultrasonic parameters, the attenuation and the frequency shift. Both parameters are used as a practical approach to define whether the coated sensor will meet the requirements to work properly in the sensor system. The frequency shift, which is directly related to the mass deposited and the thickness of the deposited layer, provides information about the mass loaded upon the sensor surface. The attenuation provides information about the material distribution and homogeneity and about the viscoelastic properties of the coating material. Therefore, the interpretation of these integral parameters is very important for the analysis of SAW coating materials.

In the first part of this work [44], based on the interpretation of the ultrasonic analysis and on the results of the CAT, some conclusions were drawn about the enhancements in the properties of the coating layers achieved by the PU polymer composites. Scheme 1 represents a pictured visualization of the coating process to support the suppositions made based on the obtained ultrasonic results. In the same way, Scheme 2 shows the situations before and after the CAT suggested to support the interpretation of the CAT effect over the sensing layers.

The results of the ultrasonic parameters obtained for the deposition of the PU polymer composites of each tested sensing polymer (PLMA, PIB, and PCTFE) before and after the application of the CAT are now presented and discussed.

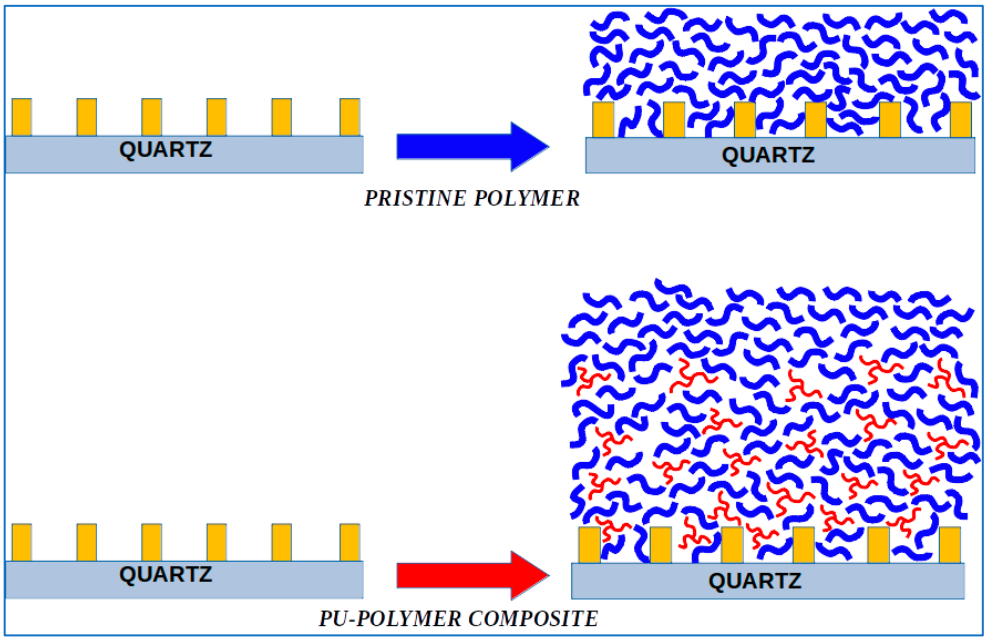

Scheme 1. Pictured representation of the suggested results of the spin coat deposition of the uncoated active area of the SAW sensor element (represented on the left side), using the pristine sensing polymer (at the upper right side) and using PU polymer composites (at the lower right side) as coating materials. The blue units represent sensing polymer macromolecules, and the red structures represent PU macromolecules.

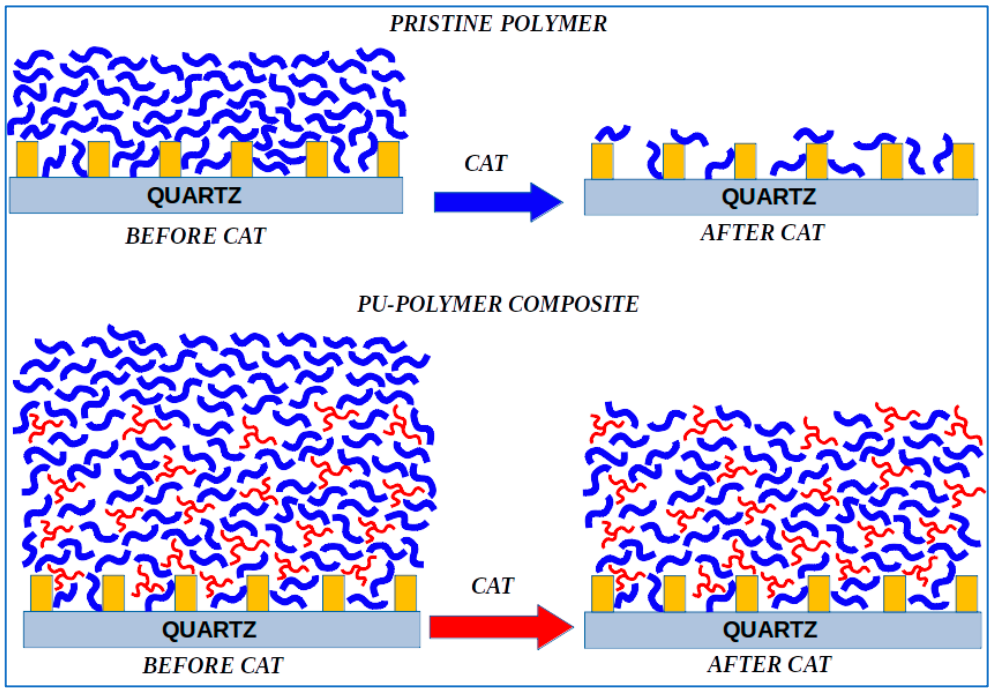

Scheme 2. Pictured representation of the suggested results for CAT for the sensors coated with the pristine sensing polymer (**above**) and those coated with the PU polymer composite (**below**). The blue units represent sensing polymer macromolecules, and the red structures represent PU macromolecules.

3.1.1. PU-PLMA Composites: Analysis of the Ultrasonic Parameters

Figure 1 presents the frequency shift, before and after the CAT, obtained for the PU polymer composites with PLMA.

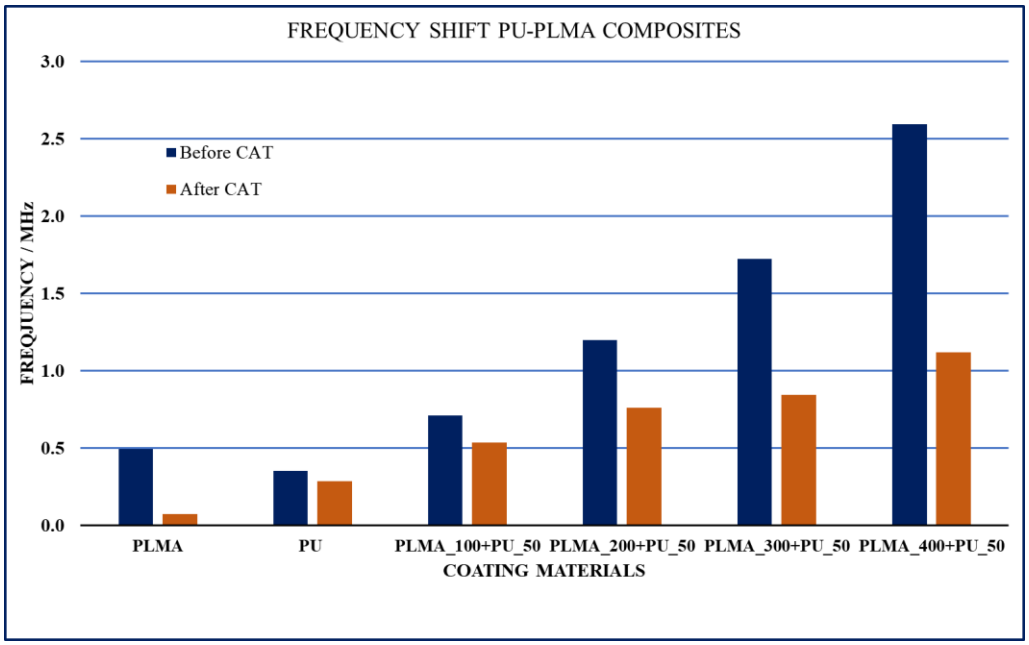

Figure 1. Frequency shift results for the coating materials with PLMA, before and after the CAT.

The results are strongly related to those obtained with the PU-PBMA composites [44]. As observed with PBMA, after the CAT, the coating layer with the pristine PLMA was almost totally removed. Contrastingly, the presence of the PU in the composites promoted an increase in the mass deposited compared with the mass deposited with the pristine polymer, indicating that a cooperative effect occurs between PU and PLMA in the process of the composite deposition.

After the CAT, a substantial quantity of the mass deposited was removed from the surface of all the PU-PLMA composites, maintaining, however, a considerable fraction of the frequency shift originally obtained. In the pristine PU deposition, a small reduction in the frequency shift after the CAT was observed. All these results are in accordance with the previous results for the PU-PBMA composites [44].

The quantitative relationship between the PLMA concentration in the coating formulations and the frequency shift obtained by the deposition of the coating materials (Table 1) and after the CAT are shown in Figure 2.

The curves of Figure 2 reproduced the profiles obtained for the same relationship in the case of PU-PBMA composites [44], which is a strong indication of the reproducibility and robustness of the method. The exact and reproducible quantitative relationship between the frequency shift due to the coating layer of the composites and the concentration of the PLMA in the coating solution, hereby indirectly represented by the volume of the sensing polymer solution added to the coating solution, and agreement with the results observed for the PU-PBMA composites suggest that the same mechanism is involved in the formation of PU polymer composites.

The results for the attenuation measured for the PU-PLMA coating materials (Table 1) are presented in Figure 3.

The results of the attenuation for the pristine PLMA and PU (Figure 3) are in accordance with those observed for the frequency shift (Figure 1) of both pristine polymers, which indicates almost complete removal of the PLMA coating, while the PU-coated sensor maintained its coating layer almost unchanged after the CAT. These observations, again, agree with those observed in the analysis of the PU-PBMA composites [44].

For the PU-PLMA composites, the results of attenuation for the coating process in Figure 3 show a regular increase in their values, which can be assigned to the successive increase in the mass deposited over the surface of the sensor elements (Figure 1). The attenuation results after the CAT for the PU-PLMA composites, however, present a tendency

toward the uniformization of their values. This observation suggests overall uniformity in terms of the coating layer structure as well as in terms of the material distribution over the sensor element surface.

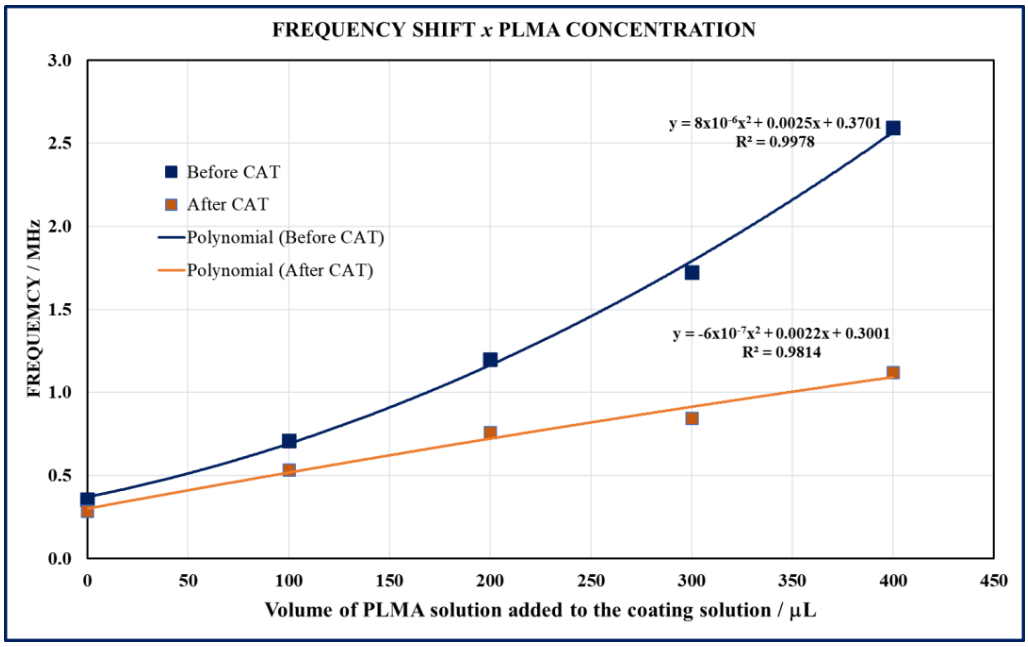

Figure 2. Frequency shift results for the coating materials with PLMA as a function of the volume of the PLMA solution added to the coating solution, before and after the CAT.

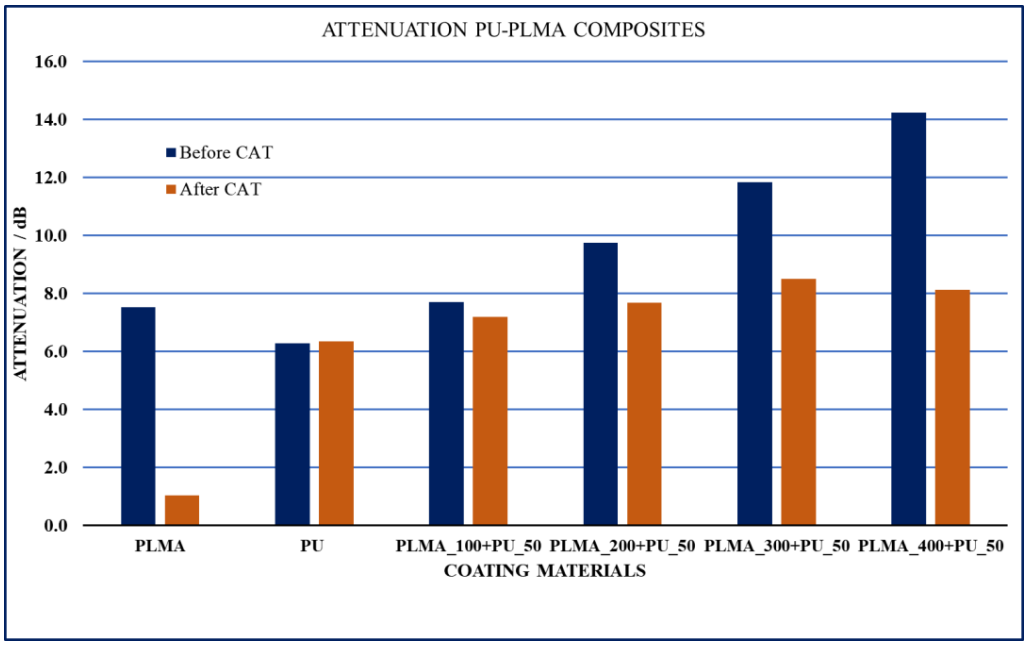

Figure 3. Attenuation results for the PU-PLMA coating materials, before and after the CAT.

Figure 4 presents the quantitative correlations of the attenuation results for the PU-PLMA composites, before and after the CAT.

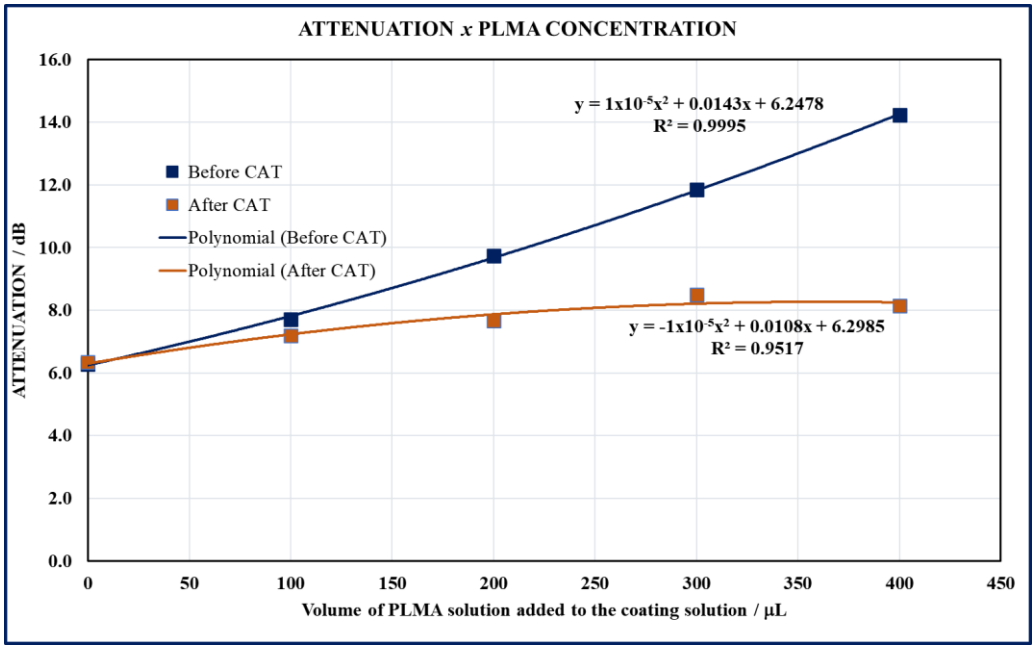

Figure 4. Attenuation results for the PU-PLMA coating materials as a function of the volume of the PLMA solution added to the coating solution, before and after the CAT.

A clear quantitative relationship between the attenuation and the PLMA concentration for the coating of the PU-PLMA composites is observed (Figure 4). The results of the quantitative correlation between the attenuation and the concentration of the PLMA in the composites confirm the previous statements about the homogeneity in terms of the structure and material distribution, reflected by the regular increase in the attenuation before the CAT, which is correlated with the increase in the mass (frequency shift) of the coating material deposited (Figure 1).

The precise quantitative correlation of the attenuation observed after the CAT (Figure 4) confirms the tendency toward alike structures after immersion in the organic solvent. This can be inferred by the similarity of the attenuation values obtained for the PU-PLMA composites after the CAT (Figure 4), strongly suggesting a high similarity of the properties of the remaining PU-PLMA composite coating layers. A possible interpretation for this observation is that after the removal of mass from the PU-PLMA coating layers by the CAT (Figure 1), the remaining coating layers tend toward more similar structures, presenting, therefore, more similar attenuation values. This tendency can be seen in the profile of the attenuation after the CAT, presented in Figure 4.

The same behavior for the attenuation before and after the CAT was observed for the PU-PBMA coating materials [44]. Based on the present results and considering the PU as the one responsible for the adhesion, chemical resistance, and support of the remaining structure of the coating layer after the application of the CAT, it could be expected that the structures of the remaining coating layers become more alike after the CAT. After the removal of the excess of the nonbonded sensing polymer, the "CAT-resistant" PU-PLMA composite structure will remain as the coating layer, and its structure will be very similar.

The comparison of the results for the PU-PBMA and PU-PLMA composites as coating materials for the SAW sensor technology provided an interesting scenario because while the two sensing polymers are made of the same backbone, they do differ by their side radicals (butyl and lauryl, respectively). This difference in the structure of the sensing polymers did not present any distinction in the behavior of the ultrasonic parameters of the coating process of the SAW sensor elements. The results before and after the CAT presented the same behavior for both sensing polymers, including the obtention of very similar profiles for the quantitative relationship of the ultrasonic parameters in terms of the concentration

of the sensing polymer in the coating solution. In future work, the absolute effect of the structure of the sensing polymers in the coating materials' properties will be addressed.

3.1.2. PU-PIB Composites: Analysis of the Ultrasonic Parameters

PIB has a completely different chemical structure from the previously analyzed polyacrylate polymers. PIB has a fully aliphatic hydrocarbon structure and the absence of any organic functional group, heteroatoms, or aromatic radicals in its structure accord an apolar character to this polymer.

Figure 5 shows the results of the frequency shift for the PU-PIB coating materials (Table 2), before and after the CAT.

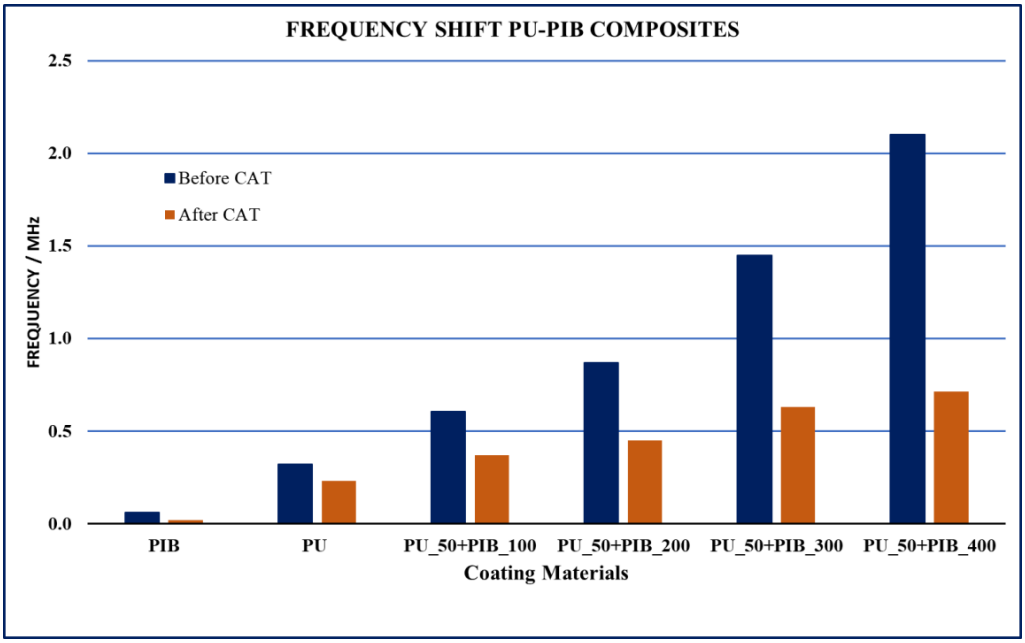

Figure 5. Frequency shift results for the PU-PIB coating materials, before and after the CAT.

The result for the pristine PU was the same as the one observed in the previous experiments where the polymer showed a deposition of approximately to 0.5 MHz of frequency shift and a little loss of this value after the CAT. For the pristine PIB, a considerable lowering of the frequency shift was observed compared with that observed for the PLMA (Figure 1). This result may be explained by two reasons: first, the lower mass of the PIB in the coating solutions (Table 2), and second, the lack of affinity of the polymer to the surface of the SAW sensor element since the lowering in the frequency shift was not proportional to the reduction in concentration compared with the previous polymer analyzed (Figure 1).

The coating layer of the pristine PIB was almost completely washed out of the surface of the SAW sensor element after the CAT, while the results for the composites went in a completely different direction. For the coating of the PU-PIB composites, the frequency shift results presented similar values to those obtained for the PU-PLMA composites, even though the pristine polymers presented very distinct values of frequency shift (Figures 1 and 5) and despite the fact that the PIB concentration in the composites was half that of PLMA (Tables 1 and 2).

These results emphasize the role played by the PU in the formation of the composites. Even though PIB possesses a quite distinct chemical structure, and, therefore, different chemical affinities than the polymetacrylate polymers previously analyzed, its association with PU gives rise to composites that show the same properties as coating materials of the PU composites of the previous sensing polymers.

Figures 1 and 5 show that the behavior of the frequency shift in the PU composites with both polymers before the CAT is very similar. These results indicate that PU provides,

at the same time, the formation of an aggregate with the sensing polymer, enhancing the mass of the sensing polymer available for the interaction with the analytes, and it enhances the adhesion of the composites to the surface even though the sensing polymer presents a lack of affinity and consequent poor adhesion to the surface of the SAW sensor element.

The results after the CAT show a similarity in the behavior of the PU-PLMA and PU-PIB composites (Figures 1 and 5). Although the sensing polymers are chemically quite distinct, the similarity observed in their behavior suggests that the PU composites are probably formed by the same mechanism. In turn, this is an indication that the methodology for the formation of PU polymer composites is a general procedure for the sensitization of SAW sensors with polymeric coating layers, independently of the chemical nature of the sensing polymer used.

The quantitative relationships of the frequency shift as a function of the PIB concentration in the coating solution, before and after the CAT, are presented in Figure 6.

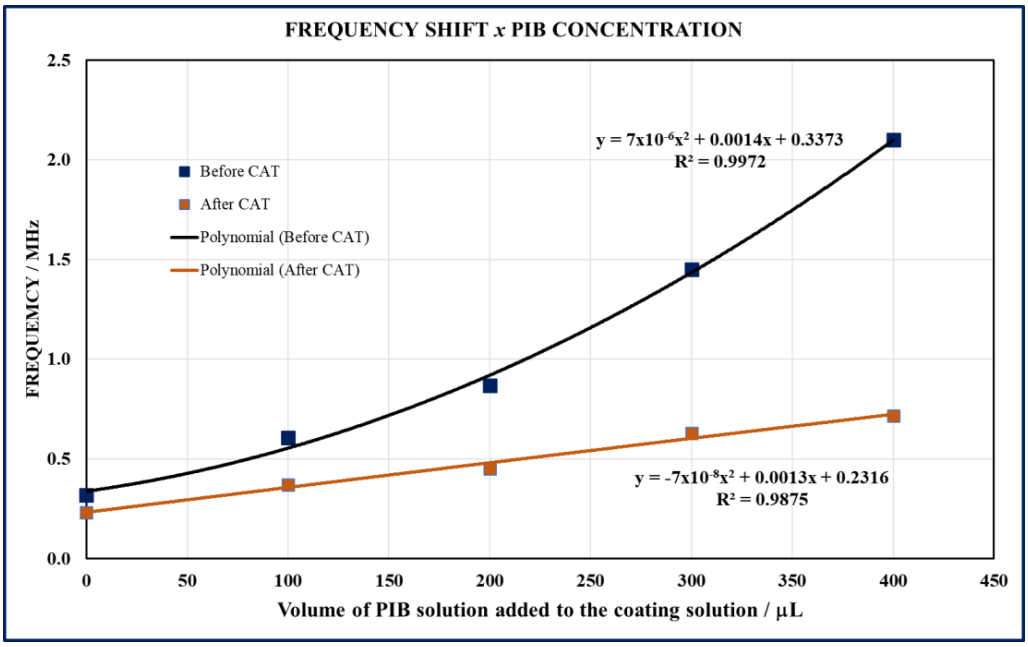

Figure 6. Frequency shift results for the coating materials with PIB as a function of the volume of the PIB solution added to the coating solution, before and after the CAT.

The profiles in Figure 6 are similar to those obtained for the PU-PLMA composites (Figure 2). Even the determination coefficients are in great agreement with both results, confirming the robustness of the coating process and the procedures of the CAT. The reproducibility of the profiles reinforces the argument that the formation of the PU polymer composites follows the same mechanism for both polymers, which is remarkable, considering the constitutional differences between PLMA and PIB.

The results after the CAT follow the same profile observed for the PU-PLMA composites (Figure 6), which is also an indication that the formation of the composites follows the same mechanism, which, in turn, could lead to the formation of composites with similar structures but with quite different compositions, and, consequently, with differences in their properties like their viscoelastic behavior and their interactions with the analytes, for example.

The analysis of the attenuation provides more insights into the properties of the PU-PIB composites. The results of attenuation before and after the CAT are shown in Figure 7.

The first important observation in Figure 7 is the attenuation of the pristine PIB coating layer, which presents a similar attenuation to that observed by the pristine PLMA (Figure 3) but shows a lower frequency shift than that observed with PLMA. In other words, it means

that less mass of the PIB deposited leads to a comparable value of attenuation to that obtained with a higher mass of PLMA.

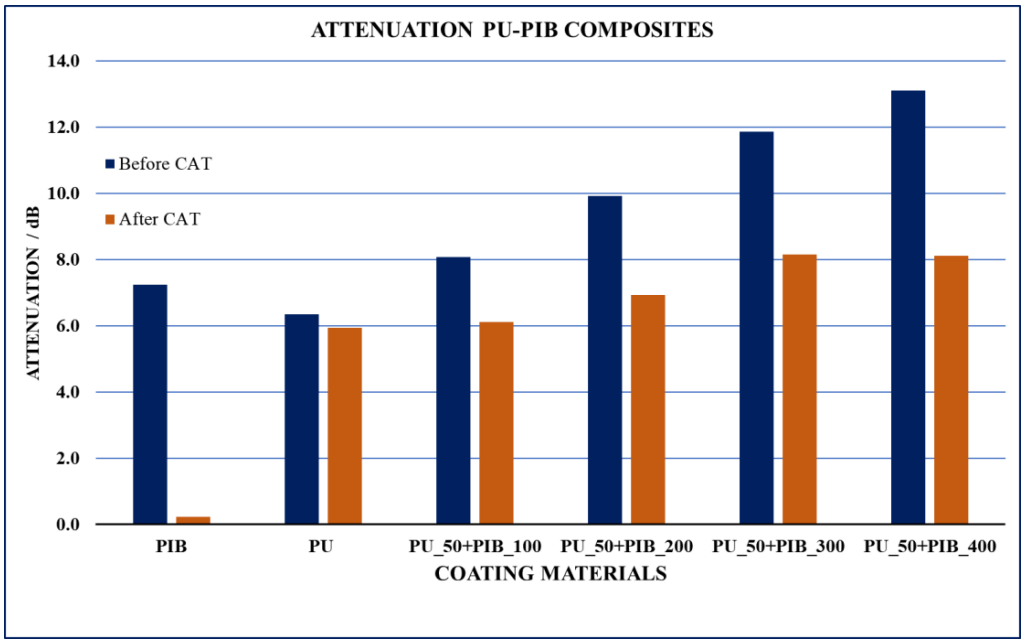

Figure 7. Attenuation results for the PU-PIB coating materials with PIB, before and after the CAT.

This observation should be interpreted as a difference in the intrinsic properties of the coating materials since a possible increase in the attenuation due to an irregular material distribution by the deposition has not been found so far. The reason is, therefore, in the differences in the constitution of the coating materials, which has a direct influence on the attenuation.

Again, for the pristine PU coating, the results reproduced the behavior observed in all the previous experiments. The results for the PU-PIB composites (Figure 7) reproduced the general behavior observed with the other PU polymer composites analyzed when the increase in the concentration of the sensing polymer in the coating solution promoted an increase in the frequency shift, which, in turn, manifested itself as an increase in the attenuation values.

After the CAT, the results for the PU-PIB composites presented the same tendency toward uniformization in terms of the structure of their remaining coating layer, as previously observed for PLMA (Figure 3). The reproduction of the relative behavior observed for the PU composites containing PLMA and PIB reinforces the argument that the same mechanism is involved in the formation of the composites and in its deposition on the surface of the SAW sensor elements.

Figure 8 shows the quantitative relationship between the attenuation and the PIB concentration of the coating solution.

The attenuation measured for the coating layers obtained with the PU-PIB composites also shows an exact quantitative relationship with the PIB concentration in the coating solution before the CAT; however, the profile of the correlation was different than that observed for PLMA (Figure 4). The difference in the profiles arises from the differences in the constitution of the sensing polymers in the coating materials. As PIB has a quite different chemical constitution than that of the polyacrylate sensing polymers previously analyzed, the results of the attenuation reflect the differences in the properties between the sensing materials of each sensing polymer by producing different profiles for the attenuation for the respective PU composites as a function of the sensing polymer concentration.

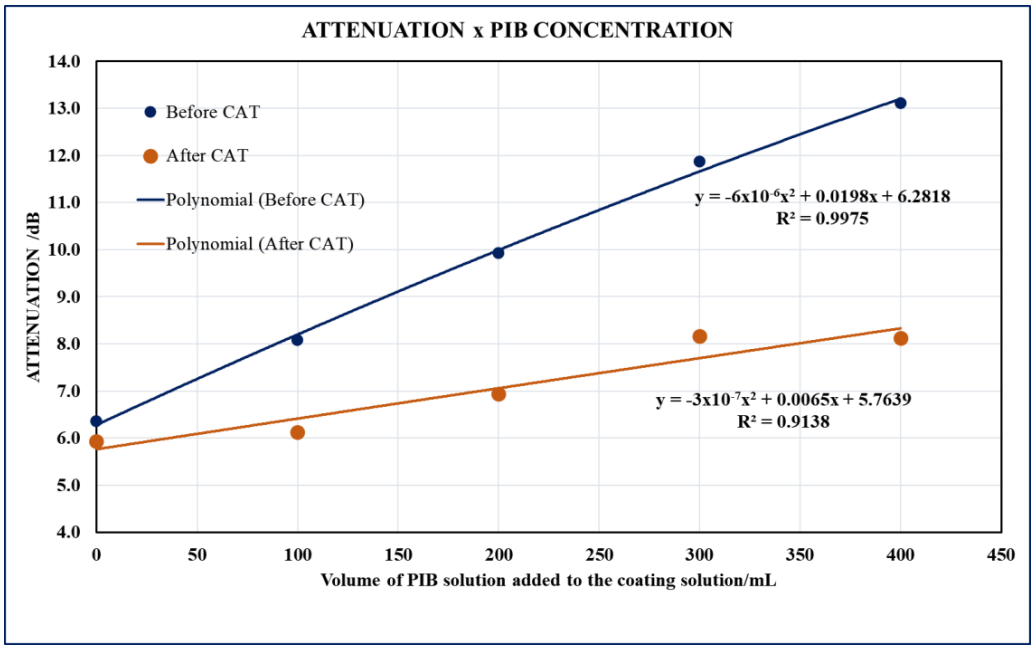

Figure 8. Attenuation results for the PU-PIB coating materials as a function of the volume of the PIB solution added to the coating solution, before and after the CAT.

The profiles obtained for the attenuation after the CAT for the PU-PIB composites are more alike to those observed for the PU-PLMA coating materials and both coating materials show the tendency toward uniformization of the structure of their remaining coating layers (Figure 4).

3.1.3. PU-PCTFE Composites: Analysis of the Ultrasonic Parameters

PCTFE-Poly(chlorotrifluoroethylene-co-vinylidene fluoride)—is a highly halogenated polymer with the general formula $[CF_2CF(Cl)]_x(CH_2CF_2)_y$. Considering its constitution, it is important to evaluate the behavior of its combinations with PU as coating materials. The homogeneity of the structures of the resulting PU-PCTFE composites (Table 3) and the uniformity of the material distribution by the coating process as well as the adhesion of the resulting coating layers to the highly polished quartz surface of the SAW piezoelectric element, with its interdigitated electrode structure, together with the sensor responses of the coating materials of the PU composites of this polymer, are now analyzed to confirm the general application of the methodology.

Figure 9 presents the frequency shifts achieved by the deposition of the pristine polymers (PCTFE and PU) and the PU-PCTFE composites (Table 3), before and after the CAT.

The result of the coating with pristine PU can be taken as the control of the coating process methodology and gives the same results before and after the CAT (Figure 9), as observed for all the other results previously analyzed, validating the coating process in the experiments with PCTFE.

The results of the frequency shift due to the coating (corresponding to the results before the CAT) show consistently higher values either for the pristine PCTFE or for its PU composites, in comparison with all the other PU polymer composites previously analyzed (Figures 1 and 5). Considering that the conditions of the coating procedure were the same for all the experiments, a possible explanation for increasing the mass observed by the coating with PCTFE and its corresponding PU composites could be a very favorable interaction between these materials and the surface of the sensor element, which would cause more mass to be retained on the surface after the spin coating process. This hypothesis will be discussed along with the further results.

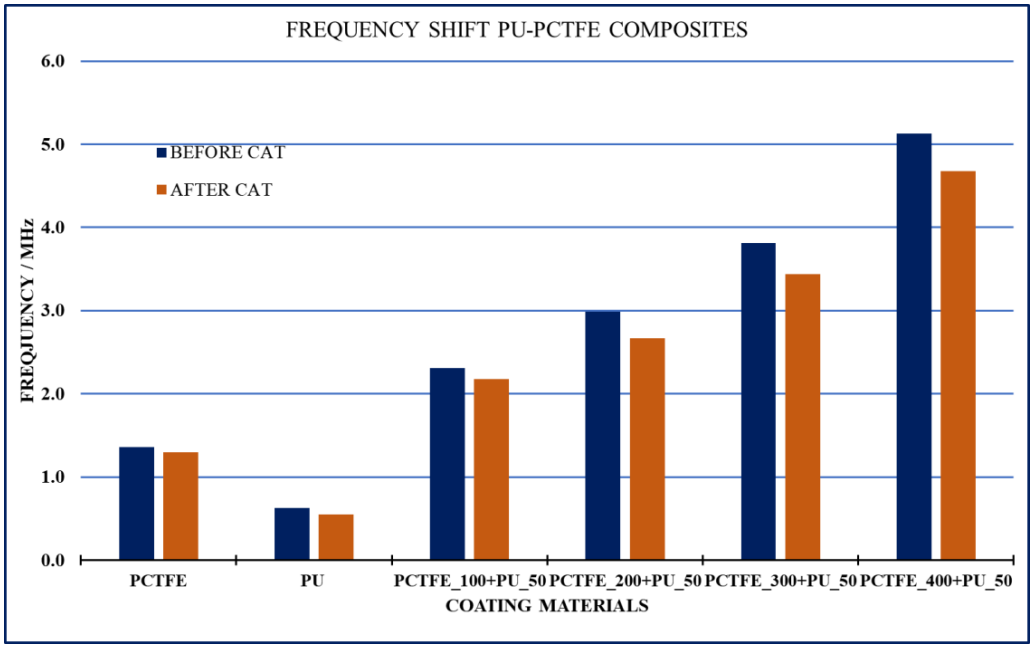

Figure 9. Frequency shift achieved with PCTFE, PU and the PU-PCTFE composite coatings, before and after the CAT.

Another reason could be due to a higher density of the PCTFE and, consequently, of its PU composites, leading to a higher mass deposited for the same volume of the coating layer. Indeed, the density of the PCTFE is approximately double that of the other polymers analyzed, which probably accounts for the significantly higher results of frequency shift observed for all the coating materials containing PCTFE from Table 3.

The results for the frequency shift after the CAT for the PCTFE and its PU composites were also distinct compared with those observed in the previous experiments (Figures 1 and 5). The pristine PCTFE preserved almost all its original value of frequency shift due to the coating, a quite distinct result in comparison with all the other polymers and PU composites, except for those of pristine PU. All the coatings with the PU-PCTFE composites also showed a significantly lower reduction in the frequency shift after the CAT than those observed in the PBMA, PLMA, and PIB experiments.

These observations can be visualized in Figure 10 where the frequency shift values before and after the CAT are plotted as a function of the volume of the polymer solution in coating solutions.

The profiles in Figure 10 are different than those obtained for PLMA and PIB (Figures 2 and 6, respectively) and clearly show a different behavior of the PU-PCTFE composites before and after the CAT.

The results for the pristine PCTFE (Figure 9) where the difference in the frequency shift before and after the CAT was much smaller than that observed for the other polymers (Figures 1 and 5) could support the hypothesis of a stronger interaction of PCTFE with the SAW sensor element surface, as mentioned before, which could lead to less removal of mass from the coating layer by the CAT. The removal of PCTFE from its coating layer is much less than that observed for all the other polymers analyzed, except for PU.

In the same sense, the higher results of the frequency shift for the PU-PCTFE composites after the CAT could be explained by a favorable interaction between the PCTFE and the PU, which, in turn, increases the interaction with the surface of the SAW sensor element when compared with that observed for the pristine PCTFE. This leads the composites to be more stable with respect to the CAT, causing less removal of mass from the coating layers of the PU-PCTFE composite.

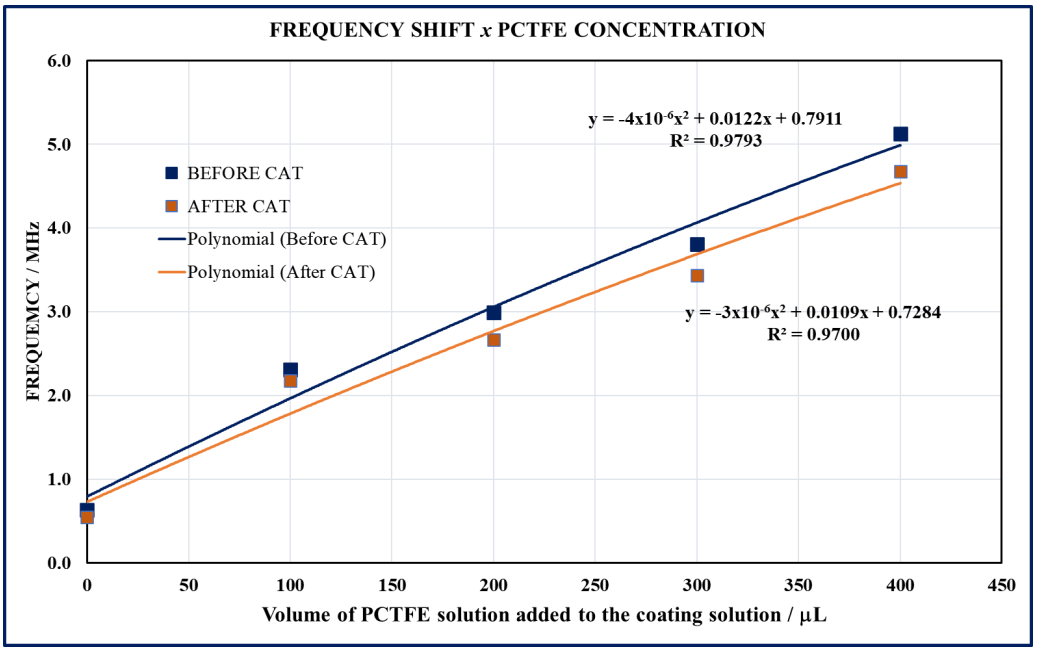

Figure 10. Frequency shift results for the PU-PCTFE coating materials as a function of the volume of the PCTFE solution added to the coating solution, before and after the CAT.

The results of the attenuation for the resulting coating layers with the PCTFE-based coating materials are shown in Figure 11.

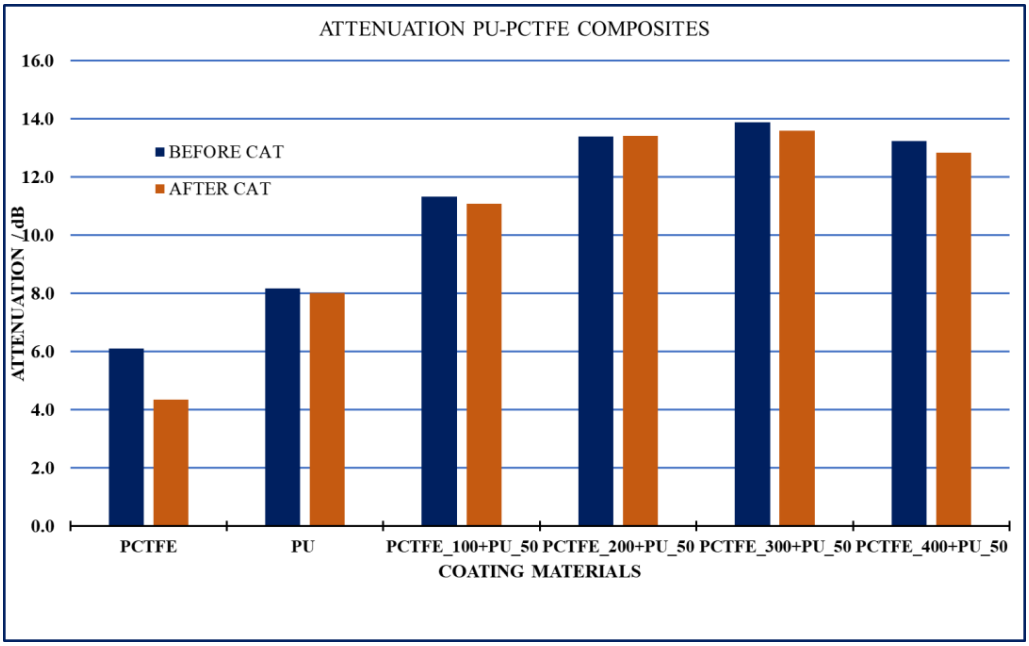

Figure 11. Attenuation results for the PU-PCTFE coating materials, before and after the CAT.

The results of the attenuation presented in Figure 11 reveal a more significant effect of the CAT on the coating with pristine PCTFE, wherethe reduction in the attenuation after the CAT was more significant than that observed in the pristine PU. In general, the reduction in the attenuation suggests that after the CAT, the coating layer tends to show a more uniform structure, which, could be achieved by the removal of polymer units that were loose in the structure of the coating layer. These loose polymer units on the coating structure shall be responsible for a higher energy dispersion of the surface wave oscillation.

The attenuation values of pristine PU after the CAT reproduced the same results as those observed in the previous experiment with the other polymers (Figures 3 and 7).

The attenuation results for the PU-PCTFE composites (Figure 11) presented the same behavior as those for the other polymers, PLMA and PIB (Figures 3 and 7) but showed much less influence of the CAT. The attenuation of the PU-PCTFE composites presented the same tendency toward the achievement of uniformity in the coating layers with the increment of the concentration of the PCTFE in the composites, as observed for all the PU polymer composites previously analyzed.

Figure 12 presents the quantitative relationship between the attenuation and the volume added of the polymeric solution to the coating solution for the PU-PCTFE composites, before and after the CAT.

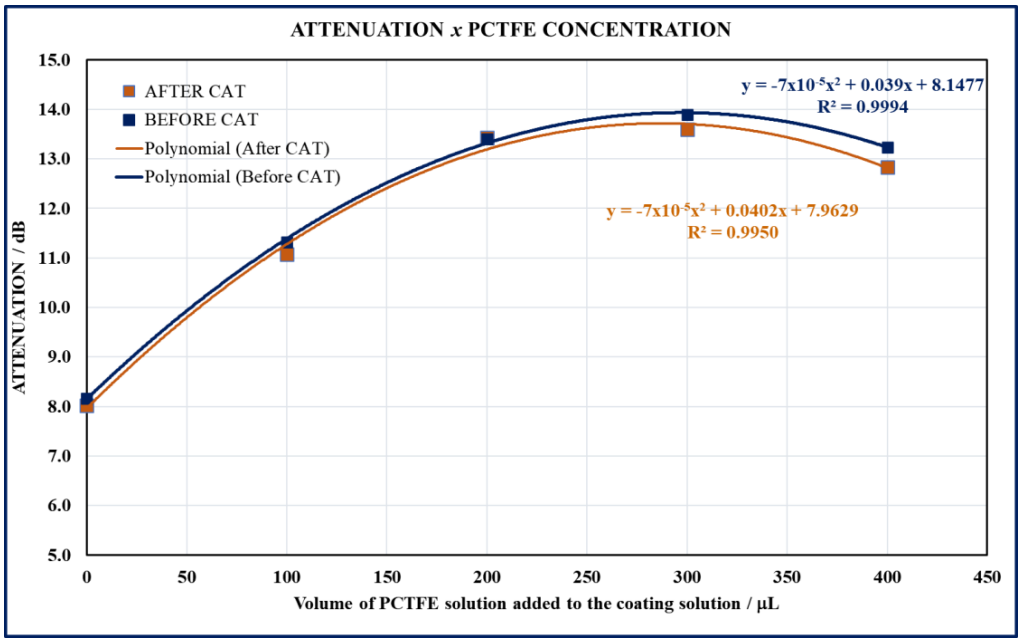

Figure 12. Attenuation results for the PU-PCFE coating materials as a function of the volume of the PCTFE solution added to the coating solution, before and after the CAT.

The profiles in Figure 12 are very exact and show a very clear quantitative correlation between the PCTFE concentration in the composite and the attenuation values. Much less influence of the CAT on the structure of the resulting PU-PCTFE composites can be clearly seen from the results of the attenuation, in this case presenting a very distinct behavior from those observed so far. It is also remarkable that the structure of the coating with pristine PU (corresponding to the zero volume in Figure 12) is so closely correlated with those of the PU-PCTFE composites. This fact significatively suggests that the structure formed by the PU polymer composites is strongly correlated with that of the pristine PU, supporting the role proposed for PU in the mechanism of the formation of the PU polymer composites [44].

Although the results in Figure 12 show an exact correlation between the attenuation and the concentration of the PCTFE, as was also observed in the previously analyzed PU polymer composites (Figures 4 and 8), the profiles obtained for the composites of the three sensing polymers analyzed are quite distinct. This fact strongly suggests that even though the mechanism of formation seems to be the same and independent of the chemical nature of the sensing polymers used to form the composites with PU, the resulting structures of each distinct PU polymer combination will be quite different. The application of the methodology provided a reliable production of fully operational SAW sensors, and the analysis of the ultrasonic parameters before and after the CAT was able to characterize and differentiate each type of the PU polymer composites. The results demonstrate that

the method is very robust and reproducible, minimizing the errors in the production of the sensors and therefore, reducing the significant cost of the loss of the expensive SAW piezoelectric quartz elements.

3.2. Analysis of the Relative Sensor Responses

The analysis of the relative sensor responses reveals the correlation between the nature of the composite coating materials of PU with varying quantities of the sensing polymer and their interaction with a given analyte from the gas phase. Once the results of the interaction with the analytes are directly correlated with the structure and the chemical composition of the coating layers obtained with the PU polymer coating materials, the relative sensor responses should be, therefore, correlated with the correspondent results of the ultrasonic parameters of the respective coating material. As the analyses of the sensing responses of the PU-polymer composites will be addressed in more detail in the sequence of this work, the analysis of the relative sensor responses will be presented for two analytes, chloroform and p-xylene, for the characterization of the PU polymer coating materials used in this work regarding their relative SAW sensor responses.

Figure 13 presents the results of the sensor responses to chloroform as the analyte for the PU-PLMA coating materials, before and after the CAT.

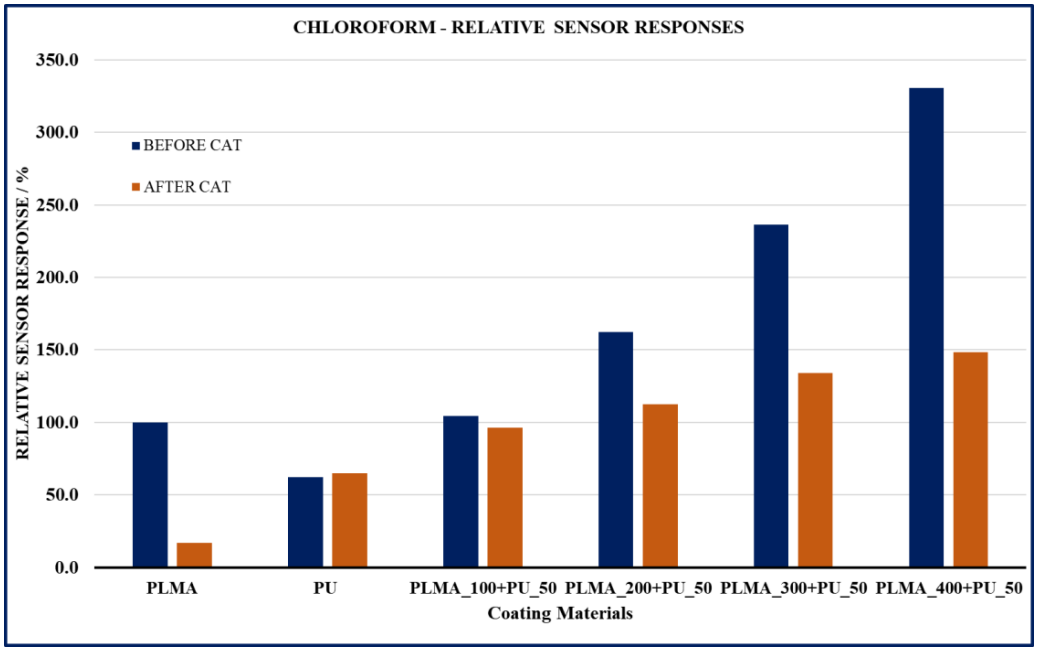

Figure 13. Relative sensor responses of the PU-PLMA coating materials to chloroform as the analyte, before and after the CAT.

The results of the relative sensor responses to the chloroform as the analyte in Figure 13 are in accordance with those of the frequency shift results for the PU-PLMA composites (Figure 1), reproducing the same behavior before and after the CAT. The higher values of the relative sensor responses obtained before the CAT indicate an increasing capacity of sorption by the composite coating materials with the increment of the sensing polymer in the composite, in agreement with the increase in the frequency shift observed (Figure 1). This fact confirms the role of the sensing polymer in the PU polymer composite coating materials as the one responsible for the responses of the SAW sensors and the sorption capacity of the analytes from the gas phase.

The relative sensor responses of the pristine PLMA as well as of the coating layers of the PU-PLMA composite coating materials originally deposited were affected by the CAT, showing the same behavior as that observed for the frequency shift (Figure 1). The pattern showed by the relative sensor responses to chloroform after the CAT (Figure 13)

also suggest the same tendency toward the uniformity of the layer structure observed after the CAT with the PU-PLMA composites in the ultrasonic results (Figures 1–4).

These statements can be visualized in the graphic of the relative sensor responses as a function of the PLMA concentration in the coating solution (Figure 14), expressed by the volume of its polymer solution.

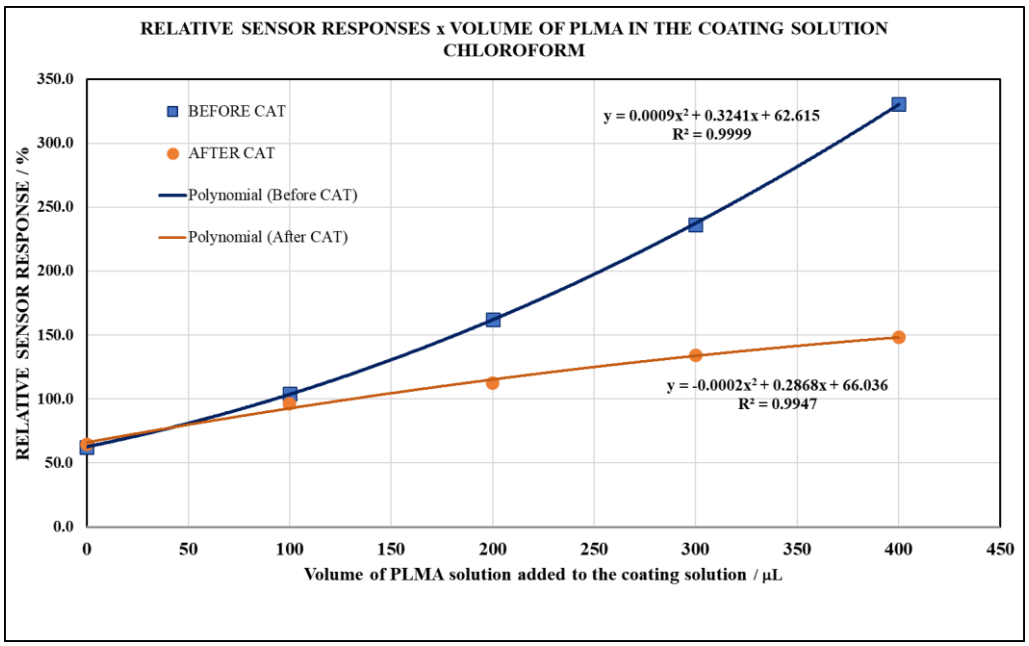

Figure 14. Relative sensor responses to chloroform as the analyte as a function of the volume of the PLMA solution added to the coating solution, before and after the CAT.

Very exact quantitative relationships regarding the content of the sensing polymer in the composites were also obtained for the relative sensor responses to chloroform, before and after the CAT (Figure 14). These correlations are in perfect agreement with the quantitative profiles obtained for the frequency shift and the attenuation for the PU-PLMA composites (Figures 2 and 4). These observations strongly suggest that the sensing mechanism is strongly related to the ultrasonic parameters. The same overall behavior of the ultrasonic parameters and their correlation to the relative sensor responses observed for the PU-PLMA coating materials were observed for the coating materials of PU-PBMA [44], suggesting that the same mechanism for the formation of the PU-polymer composite coating layers is involved, resulting in coating layers with similar structures generating similar profiles for the interaction with the analytes.

The relative sensor responses for the PU-PIB composites before and after the CAT are shown in Figure 15.

Here again, the same behavior as that for the PU-PLMA composites was observed. The relative sensor responses to chloroform as the analyte for the PU-PIB coating materials also agree with the behavior of its ultrasonic parameters (Figures 5 and 7).

Figure 16 presents the quantitative relationship between the relative sensor responses to chloroform as the analyte as a function of the concentration of the sensing polymer in the PU-PIB composites.

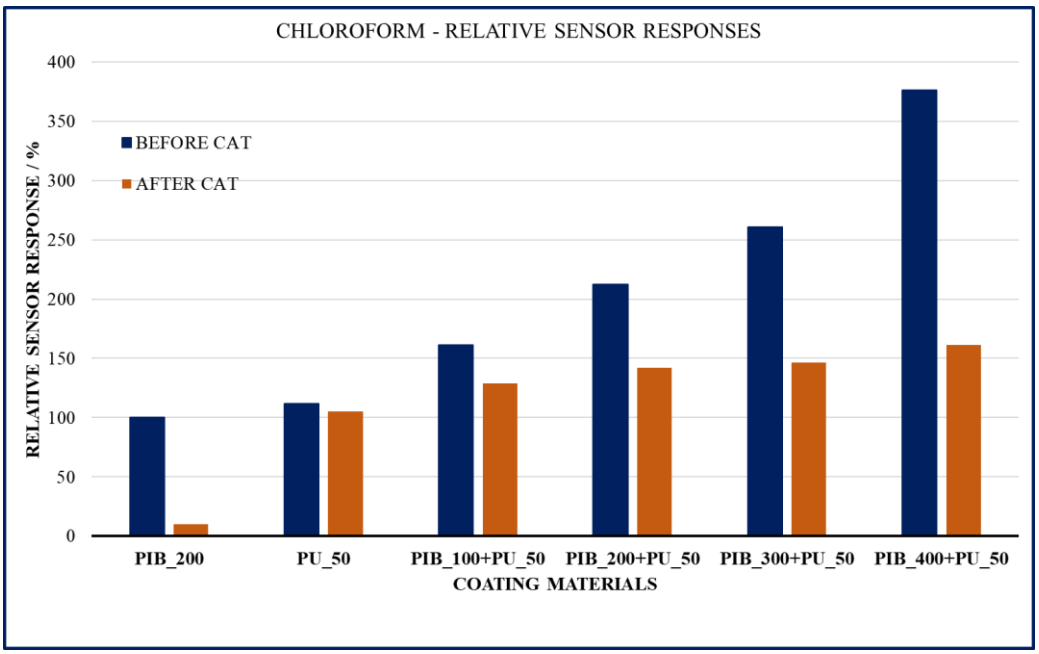

Figure 15. Relative sensor responses of the PU-PIB coating materials to chloroform as the analyte, before and after the CAT.

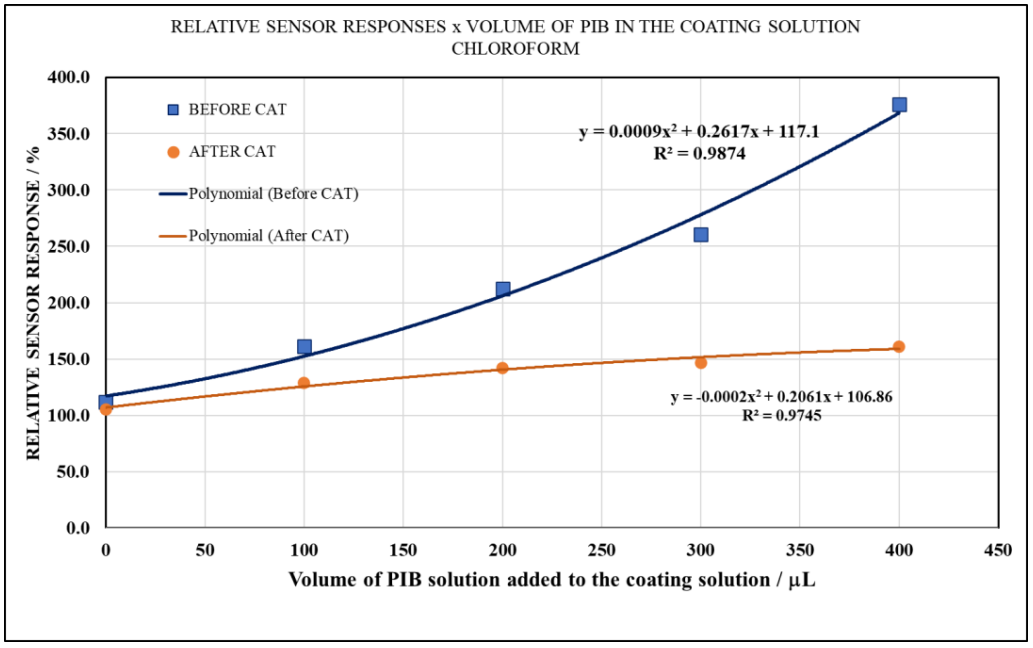

Figure 16. Relative sensor responses to chloroform as the analyte as a function of the volume of the PIB solution added to the coating solution, before and after the CAT.

The exact quantitative relationship obtained for the relative sensor responses of the PU-PIB coating materials (Figure 16) reproduces almost exactly the profile obtained for the frequency shift, and all the observations made for the PU-PLMA coating materials can be applied to the case of the PU-PIB coating materials. The results for both polymer composites agree with the ultrasonic parameters, and in both cases, the behavior was very alike, strongly suggesting that the formation of the PU-PIB, PU-PLMA and PU-PBMA composites follow the same mechanism as that postulated for the formation of the PU-PBMA composites [44].

Figure 17 shows the relative sensor responses to chloroform as the analyte for the PU-PCTFE composites, before and after the CAT.

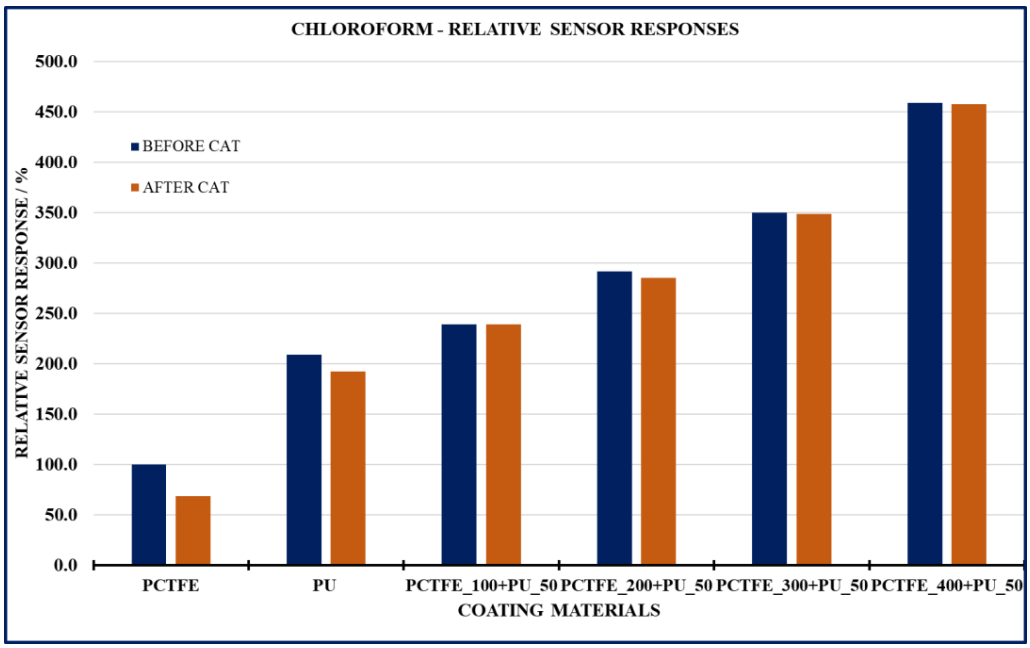

Figure 17. Relative sensor responses of the PU-PCTFE coating materials to chloroform as the analyte, before and after the CAT.

The relative sensor responses of the PU-PCTFE composites to chloroform follow the same pattern as the results for the corresponding frequency shifts measured for these coating materials (Figure 9), reproducing once more the same behavior observed for the previous two PU polymer composites. The results of the relative sensor responses before and after the CAT agree with the frequency shift results, confirming the argument about the resulting composite structures and the respective resulting effect of the CAT on the original deposited sensing layers for this type of composites.

Additionally, the analysis of the quantitative relationship observed between the relative sensor responses to chloroform and the concentration of the sensing polymer in the composite presented in Figure 18 show very exact correlations before and after the CAT.

The exactness of the correlations and their agreement with the frequency shift patterns indicate that the formation of the sensing layers of the composites follows the same mechanism, and their structures are correlated with the concentration of the sensing polymer in the composites. The same was observed for all the composites analyzed so far, for all the families of composites, even though they are made of chemically distinct sensing polymers in combination with PU.

The relative sensor responses to chloroform as the analyte were very high for all sensing layers of the three PU polymer composites analyzed, which denotes a very favorable and intense interaction.

The next analysis of relative sensor responses of the coating materials uses p-xylene as the analyte. Figure 19 presents the relative sensor response patterns for the PU-PLMA coating materials to p-xylene as the analyte, before and after the CAT.

Despite the fact that the relative sensor responses were lower for p-xylene than those obtained with chloroform (Figure 13), the same patterns for the relative sensor responses were observed for p-xylene as those obtained for the frequency shift of the PU-PLMA composites (Figure 1) and for the relative sensor response to the chloroform as the analyte (Figure 13), once again indicating the correspondence between the structures of the composites and the frequency shift parameter and their correlation with the relative sensor responses.

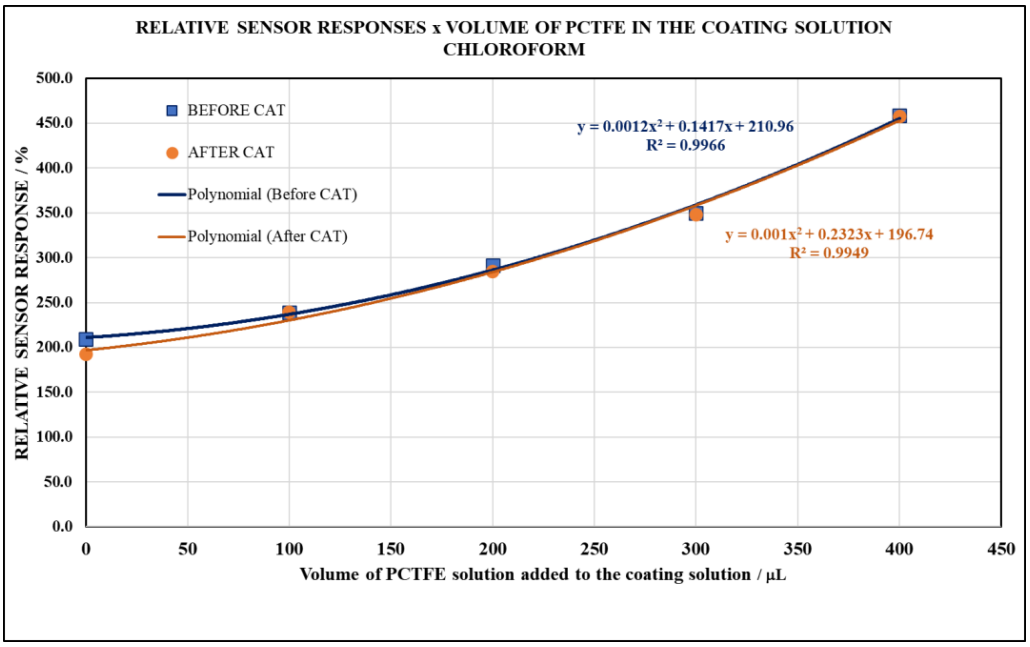

Figure 18. Relative sensor responses of the coating materials with PCTFE to chloroform as the analyte, before and after the CAT.

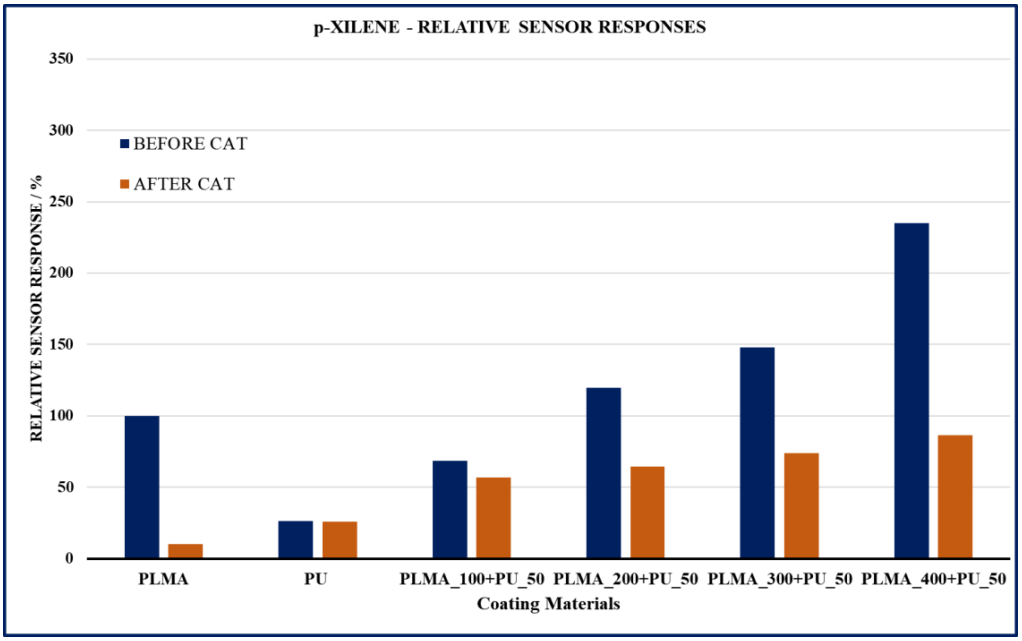

Figure 19. Relative sensor responses of the PU-PLMA coating materials to p-xylene as the analyte, before and after the CAT.

Consistently, the same profiles for the quantitative relationship between the relative sensor responses and the sensing polymer concentration in the composite were observed (Figure 20). These profiles were in perfect agreement with the quantitative profile obtained for the relationship between the frequency shift and the concentration of PLMA in the composites with PU (Figure 2).

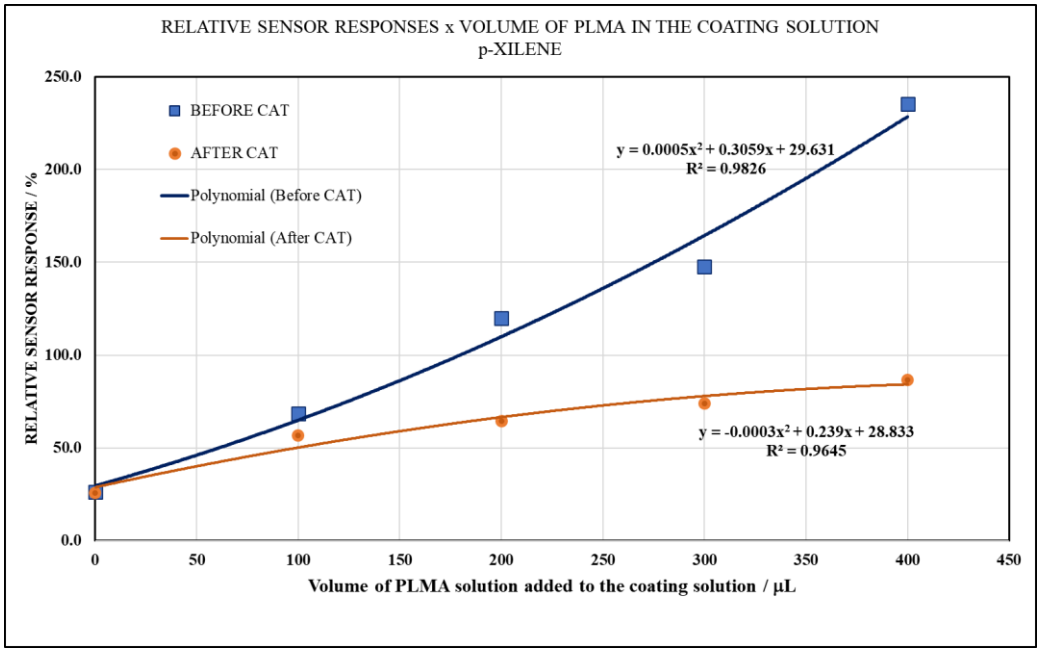

Figure 20. Relative sensor responses of p-xylene as the analyte as a function of the volume of the PLMA solution added to the coating solution, before and after the CAT.

Figure 21 shows the results for the relative sensor responses of the PU-PIB composites as the coating materials.

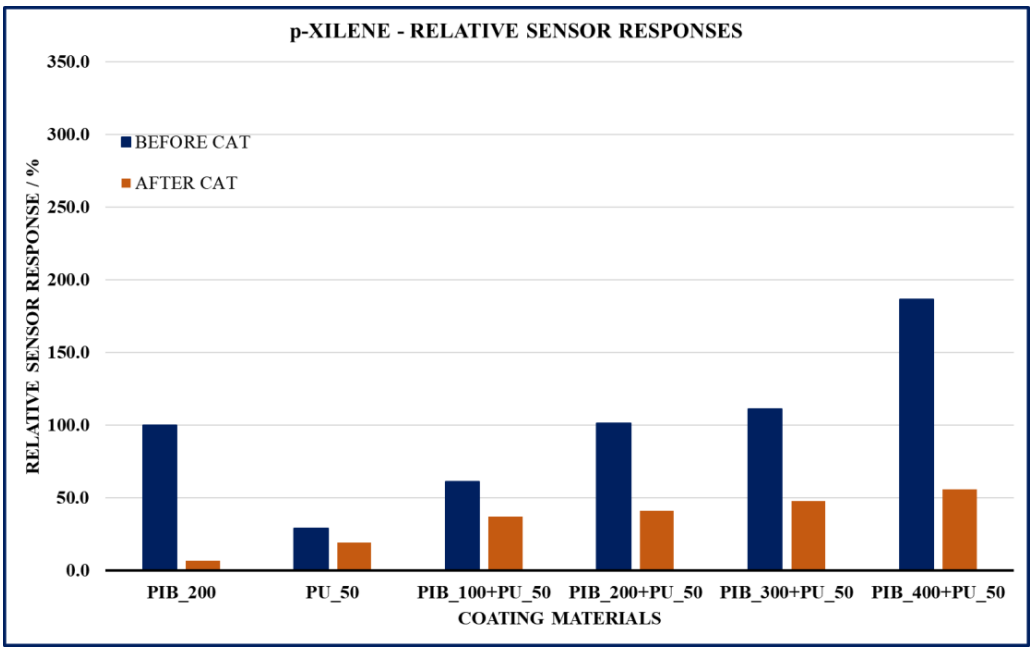

Figure 21. Relative sensor responses of the PU-PIB coating materials to p-xylene as the analyte, before and after the CAT.

The relative sensor responses for the p-xylene as the analyte were much lower than those measured for chloroform with the coating of the PU-PIB composites (Figure 15). The patterns of the relative sensor responses for the p-xylene for the PU-PIB composites agree with the patterns obtained for the frequency shift results for the PU-PIB composites (Figure 5).

Exact quantitative profiles for the relative sensor responses as a function of the PIB concentration in the composites were consistently obtained for the results before and after the CAT (Figure 22).

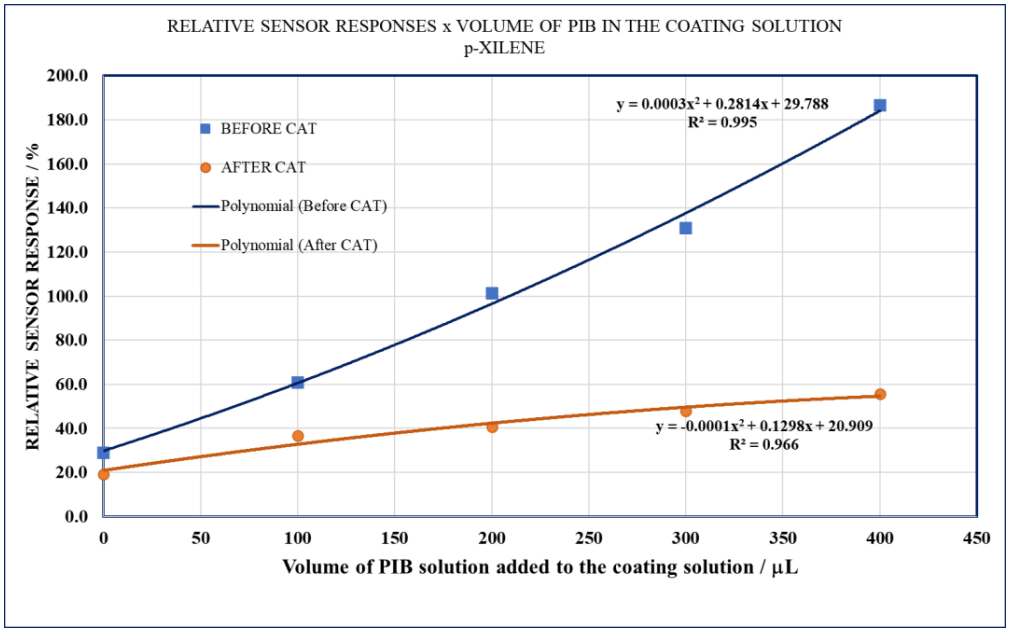

Figure 22. Relative sensor responses to p-xylene as the analyte as a function of the volume of the PIB solution added to the coating solution, before and after the CAT.

The results in Figure 22 reproduce the same profiles obtained for the quantitative relationship of the frequency shift with the PIB concentration in the PU-PIB composites (Figure 6), as observed for all the PU polymer composites investigated, strongly indicating that the process of formation of the PU-PIB composites follows the same mechanism observed for all the PU polymer composites previously analyzed.

Figure 23 presents the relative sensor responses to p-xylene obtained with the PU-PCTFE composites as coating materials.

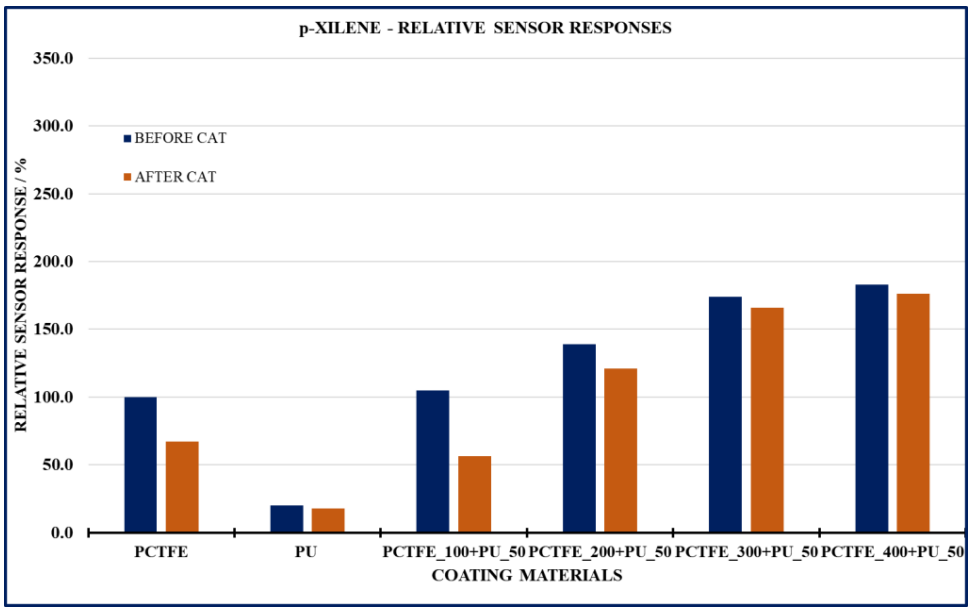

Figure 23. Relative responses of the PU-PCTFE coating material sensors to p-xylene as the analyte, before and after the CAT.

For p-xylene, the relative responses of the PU-PCTFE composite sensors (Figure 23) reproduce the same behavior observed for the results for the frequency shift for the PU-PCTFE composites (Figure 9), following the same behavior observed for the previous PU polymer composites.

The quantitative profiles, before and after the CAT, for the relative sensor responses as a function of the PCTFE concentration on the composites are presented in Figure 24.

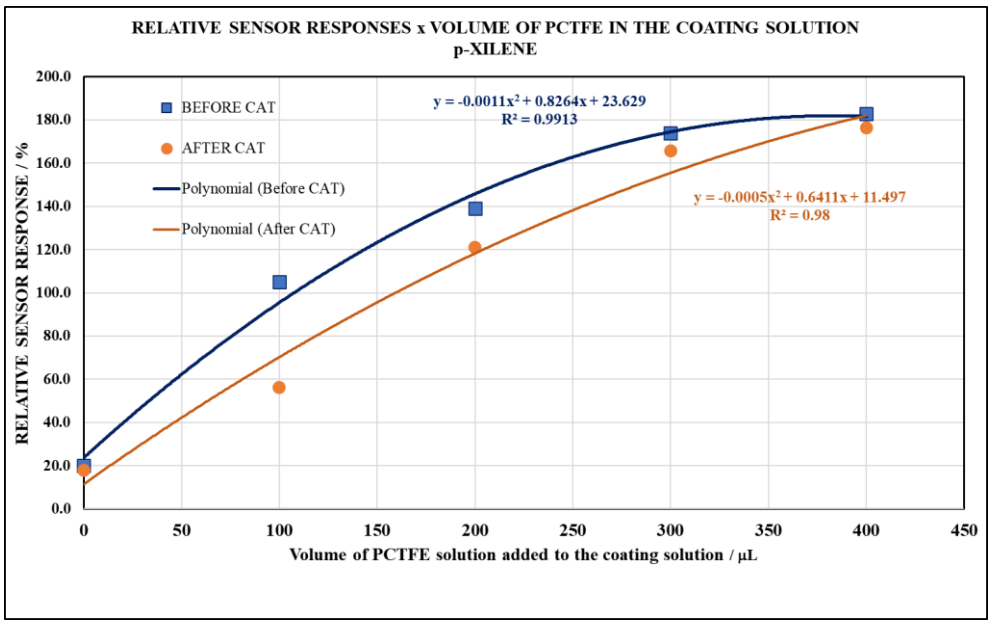

Figure 24. Relative sensor responses to p-xylene as the analyte as a function of the volume of the PCTFE solution added to the coating solution, before and after the CAT.

In the same way, the quantitative profile correlating the relative sensor responses and the concentration of PCTFE in the composites (Figure 24) resembles the quantitative profiles obtained for the frequency shift for the PU-PCTFE composite coating before and after the CAT (Figure 10).

4. Conclusions

In this part of the work, the methodology previously developed for a practical approach to produce SAW chemical sensors using PU-PBMA composites as sensing materials [44] was applied to three other different sensing polymers. The overall results of the application of the methodology for the sensitization of the SAW sensors using the PU-composite coating materials with PLMA, PIB, and PCTFE reproduced the results observed for the PU-PBMA composites [44]. All the results strongly suggest that the process of the formation of the PU polymer composites should follow the same mechanism, independent of the chemical nature of the sensing polymer used. Even though the three newly tested sensing polymers have quite different chemical structures and properties, the methodology made it possible to coat the SAW sensor element with their respective PU composites with varied compositions of the sensing polymer to obtain fully operational SAW chemical sensors. This fact is a great advantage because the method allows for the use of materials that would not be fully compatible with the gold-quartz surface of the SAW sensor element and could lead to a lack of adhesion or even dewetting of the coating material. For all the sensing polymers tested, the coating layers of the composite materials showed improved properties in comparison with the coating using the pristine polymer. All the composites, independently of their sensing polymers, showed enhanced adhesion to the sensor element surface, improved chemical resistance to the organic solvent of the CAT, and enhancement of the sensor response relative to those of the sensing pristine polymer as the coating layer. The methodology is very simple, easy to use, and low cost, and yet very robust and highly

reproducible, providing a reliable procedure for obtaining homogeneous coating layers for the SAW sensor technology, in a very controlled and reproducible way. The results confirm the possibility of the general application of the methodology, considerably expanding the possibilities of chemical sensitization for the SAW technology since virtually any polymer can be tailored to the surface to achieve the selectivity of the desired analytes.

In the sequence of this work, further correlations of the resulting structure and the properties of coating layers by the formation of the PU-polymer composites as well as the selectivity of the sensor responses as a function of the chemical nature of the composites will be addressed.

Author Contributions: Conceptualization, M.d.S.d.C. and M.R.; methodology, M.R. and A.V.; software, A.V.; formal analysis, M.D.; investigation, M.D.; data curation, M.d.S.d.C. and M.D.; writing—original draft, M.d.S.d.C.; writing—review and editing, M.d.S.d.C., M.R. and A.V.; project administration, M.R. All authors have read and agreed to the published version of the manuscript.

Funding: The authors acknowledge the support from the KIT-Publication Fund of the Karlsruhe Institute of Technology.

Institutional Review Board Statement: Not applicable.

Informed Consent Statement: Not applicable.

Data Availability Statement: The data presented in this study are available on request from the corresponding author.

Conflicts of Interest: The authors declare no conflict of interest.

References

1. Atashbar, M.; Sadek, A.; Wlodarski, W.; Sriram, S.; Bhaskaran, M.; Cheng, C.; Kaner, R.; Kalantar-Zadeh, K. Layered SAW gas sensor based on CSA synthesized polyaniline nanofiber on AlN on 64 YX $LiNbO_3$ for H_2 sensing. *Sens. Actuators B Chem.* **2009**, *138*, 85–89. [CrossRef]
2. Atashbar, M.Z.; Bazuin, B.J.; Simpeh, M.; Krishnamurthy, S. 3D FE simulation of H_2 SAW gas sensor. *Sens. Actuators B Chem.* **2005**, *111*, 213–218. [CrossRef]
3. Levit, N.; Pestov, D.; Tepper, G. High surface area polymer coatings for SAW-based chemical sensor applications. *Sens. Actuators B Chem.* **2002**, *82*, 241–249. [CrossRef]
4. Sivaramakrishnan, S.; Rajamani, R.; Smith, C.S.; McGee, K.A.; Mann, K.R.; Yamashita, N. Carbon nanotube-coated surface acoustic wave sensor for carbon dioxide sensing. *Sens. Actuators B Chem.* **2008**, *132*, 296–304. [CrossRef]
5. Maslennikova, A.V.; Zubkovb, I.L.; Sazhina, S.G. Experimental Research of SAW-Sensors Applied to Atmospheric Leak Hunting. *Russ. J. Nondestruct. Test.* **2018**, *54*, 410–418. [CrossRef]
6. Milone, A.; Monteduro, A.G.; Rizzato, S.; Leo, A.; Di Natale, C.; Kim, S.S.; Maruccio, G. Advances in Materials and Technologies for Gas Sensing from Environmental and Food Monitoring to Breath Analysis. *Adv. Sustain. Syst.* **2023**, *7*, 2200083. [CrossRef]
7. Avramov, I.D.; Voigt, A.; Rapp, M. Rayleigh SAW resonators using gold electrode structure for gas sensor applications in chemically reactive environments. *Electron. Lett.* **2005**, *41*, 450–452. [CrossRef]
8. Panneerselvam, G.; Thirumal, V.; Pandya, H.M. Review of Surface Acoustic Wave Sensors for the Detection and Identification of Toxic Environmental Gases/Vapors. *Arch. Acoust.* **2018**, *43*, 357–367.
9. Li, C.; Kan, H.; Luo, J.; Fu, C.; Zhou, J.; Liu, X.; Wang, W.; Wei, Q.; Fu, Y. A high performance surface acoustic wave visible light sensor using novel materials: Bi_2S_3 nanobelts. *RSC Adv.* **2020**, *10*, 8936–8940. [CrossRef]
10. Maboudian, R. Impact of Surface Acoustic Wave Sensors on Chemical Sciences. *ACS Sens.* **2020**, *5*, 2973–2974. [CrossRef]
11. Delsing, P.; Cleland, A.N.; Schuetz, M.J.; Knörzer, J.; Giedke, G.; Cirac, J.I.; Srinivasan, K.; Wu, M.; Balram, K.C.; Bäuerle, C.; et al. The 2019 surface acoustic waves roadmap. *J. Phys. D Appl. Phys.* **2019**, *52*, 353001. [CrossRef]
12. Mandal, D.; Banerjee, S. Surface AcousticWave (SAW) Sensors: Physics, Materials, and Applications. *Sensors* **2022**, *22*, 820. [CrossRef] [PubMed]
13. Schmitt, C.C.; Rapp, M.; Voigt, A.; de Carvalho, M.D.S. Selective Detection of Aromatic Compounds with a Re-Designed Surface Acoustic Wave Sensor System Using a Short-Packed Column. *Coatings* **2022**, *12*, 1666. [CrossRef]
14. de Carvalho, M.D.S.; Rapp, M.; Voigt, A. A New Hyphenated μTrap-GC-Surface Acoustic Wave (SAW) Based Electronic Nose for Monitoring of Coffee Quality. *AIP Conf. Proc.* **2009**, *1137*, 48–50.
15. Devkota, J.; Ohodnicki, P.R.; Greve, D.W. SAW Sensors for Chemical Vapors and Gases. *Sensors* **2017**, *17*, 801. [CrossRef]
16. Palla-Papavlu, A.; Voicu, S.I.; Dinescu, M. Sensitive Materials and Coating Technologies for Surface Acoustic-Wave Sensors. *Chemosensors* **2021**, *9*, 105. [CrossRef]

17. McGill, R.A.; Chung, R.; Chrisey, D.B.; Dorsey, P.C.; Matthews, P.; Piqué, A.; Mlsna, T.E.; Stepnowski, J.L. Performance optimization of surface acoustic wave chemical sensors. *IEEE Trans. Ultrason. Ferroelectr. Freq. Control* **1998**, *45*, 1370–1380. [CrossRef]
18. Nicolae, I.; Viespe, C.; Grigoriu, C. Nanocomposite sensitive polymeric films for SAW sensors deposited by the MAPLE direct write technique. *Sens. Actuators B* **2011**, *158*, 418–422. [CrossRef]
19. Viespe, C.; Grigoriu, C. Surface acoustic wave sensors with carbon nanotubes and SiO_2/Si nanoparticles based nanocomposites for VOC detection. *Sens. Actuators B* **2010**, *147*, 43–47. [CrossRef]
20. Sadek, A.Z.; Wlodarski, W.; Shin, K.; Kaner, R.B.; Kalantar-Zadeh, K. A polyaniline/WO_3 nanofiber composite-based ZnO/64° YX $LiNbO_3$ SAW hydrogen gas sensor. *Synth. Met.* **2008**, *158*, 29–32. [CrossRef]
21. Golany, Z.; Weisbord, I.; Abo-Jabal, M.; Manor, O.; Segal-Peretz, T. Polymer dewetting in solvent-non-solvent environment- new insights on dynamics and lithography-free patterning. *J. Colloid Interface Sci.* **2021**, *596*, 267–277. [CrossRef]
22. Xu, L.; Shi, T.; An, L. The dewetting dynamics of the polymer thin film by solvent annealing. *J. Chem. Phys.* **2008**, *129*, 044904. [CrossRef]
23. Lee, S.H.; Yoo, P.J.; Kwon, S.J.; Lee, H.H. Solvent-driven dewetting and rim instability. *J. Chem. Phys.* **2004**, *121*, 4346–4351. [CrossRef]
24. Das, A.; Mukherjee, R. Feature Size Modulation in Dewetting of Nanoparticle-Containing Ultrathin Polymer Films. *Macromolecules* **2021**, *54*, 2242–2255. [CrossRef]
25. Liu, X.; Shen, B.; Jiang, L.; Yang, H.; Jin, C.; Zhou, T. Study on SAW Methane Sensor Based on Cryptophane-A Composite Film. *Micromachines* **2023**, *14*, 266. [CrossRef]
26. Sayago, I.; Fernández, M.J.; Fontecha, J.L.; Horrillo, M.C.; Vera, C.; Obieta, I.; Bustero, I. Surface acoustic wave gas sensors based on polyisobutylene and carbon nanotube composites. *Sens. Actuators B* **2011**, *156*, 1–5. [CrossRef]
27. Pasupuleti, K.S.; Bak, N.-H.; Peta, K.R.; Kim, S.-G.; Cho, H.D.; Kim, M.-D. Enhanced sensitivity of langasite-based surface acoustic wave CO gas sensor using highly porous Ppy@PEDOT:PSS hybrid nanocomposite. *Sens. Actuators B Chem.* **2022**, *363*, 131786. [CrossRef]
28. Wang, B.; Zhou, L.; Wang, X. Surface acoustic wave sensor for formaldehyde gas detection using the multi-source spray-deposited graphene/PMMA composite film. *Front. Mater.* **2023**, *9*, 1025903. [CrossRef]
29. Viespe, C.; Miu, D. Characteristics of Surface Acoustic Wave Sensors with Nanoparticles Embedded in Polymer Sensitive Layers for VOC Detection. *Sensors* **2018**, *18*, 2401. [CrossRef]
30. Sayago, I.; Fernández, M.J.; Fontecha, J.L.; Horrillo, M.C.; Vera, C.; Obieta, I.; Bustero, I. New sensitive layers for surface acoustic wave gas sensors based on polymer and carbon nanotube composites. *Sens. Actuators B Chem.* **2012**, *175*, 67–72. [CrossRef]
31. Hung, T.-T.; Chung, M.-H.; Chiu, J.-J.; Yang, M.-W.; Tien, T.-N.; Shen, C.-Y. Poly(4-styrenesulfonic acid) doped polypyrrole/tungsten oxide/reduced graphene oxide nanocomposite films based surface acoustic wave sensors for NO sensing behavior. *Org. Electron.* **2021**, *88*, 106006. [CrossRef]
32. Constantinoiu, I.; Viespe, C. Detection of Volatile Organic Compounds Using Surface AcousticWave Sensor Based on Nanoparticles Incorporated in Polymer. *Coatings* **2019**, *9*, 373. [CrossRef]
33. Constantinoiu, I.; Viespe, C. Hydrogen Detection with SAW Polymer/Quantum Dots Sensitive Films. *Sensors* **2019**, *19*, 4481. [CrossRef] [PubMed]
34. da Silva, E.A.; Samuel, C.; Furini, L.N.; Constantino, C.J.L.; Redon, N.; Duc, C. Poly(aniline)-based ammonia sensors: Understanding the role of polyurethane on structural/morphological properties and sensing performances. *Sens. Actuators B Chem.* **2023**, *397*, 134664. [CrossRef]
35. Ren, X.; Tian, Q.; Zhu, X.; Mi, H.-Y.; Jing, X.; Dong, B.; Liu, C.; Shen, C. Multi-scale closure piezoresistive sensor with high sensitivity derived from polyurethane foam and polypyrrole nanofibers. *Chem. Eng. J.* **2023**, *474*, 145926. [CrossRef]
36. Savan, E.K.; Özcan, I.; Köytepe, S. Preparation of mesoporous carbon containing Polyurethane/Clay nanocomposite membrane based sensors for sensitive and selective determination of vitamin D_2 in urine samples. *Measurement* **2022**, *203*, 111979. [CrossRef]
37. Madbouly, A.I.; Hassanien, W.S.; Morsy, M. Tailoring the polyurethane foam/rGO/$BaTiO_3$ pressure sensor for human activities. *Diam. Relat. Mater.* **2023**, *136*, 109940. [CrossRef]
38. Hasanzadeh, I.; Eskandari, M.J.; Daneshmand, H. Polyurethane acrylate/multiwall carbon nanotube composites as temperature and gas sensors: Fabrication, characterization, and simulation. *Diam. Relat. Mater.* **2022**, *130*, 109484. [CrossRef]
39. Wan, Y.; Jiang, H.; Ren, Y.; Liu, Y.; Zhang, L.; Lei, Q.; Zhu, D.; Liu, J.; Zhang, X.; Ma, N.; et al. Photothermal self-healable polypyrrole-polyurethane sponge with dynamic covalent oximino bonds for flexible strain sensors. *Eur. Polym. J.* **2023**, *193*, 112097. [CrossRef]
40. Maeng, B.; Kim, S.; An, H.; Jung, D. A tough and stretchable colorimetric sensor based on a curcumin-loaded polyurethane electrospun fiber mat for hazardous ammonia gas detection. *Sens. Actuators B Chem.* **2023**, *394*, 134420. [CrossRef]
41. da Silva, R.; Cervini, P.; Buoro, R.M.; Cavalheiro, É.T. A new acetylene black and vegetable oil based polyurethane composite: Preparation, characterization, and its potentialities as an electroanalytical sensor. *Mater. Today Commun.* **2022**, *31*, 103691. [CrossRef]
42. Tang, Y.; Xu, Y.; Yang, J.; Song, Y.; Yin, F.; Yuan, W. Stretchable and wearable conductometric VOC sensors based on microstructured MXene/polyurethane core-sheath fibers. *Sens. Actuators B Chem.* **2021**, *346*, 130500. [CrossRef]

43. Wang, Q.; Tong, J.; Wang, N.; Chen, S.; Sheng, B. Humidity sensor of tunnel-cracked nickel@polyurethane sponge for respiratory and perspiration sensing. *Sens. Actuators B Chem.* **2020**, *330*, 129322. [CrossRef]
44. Rapp, M.; Voigt, A.; Dirschka, M.; de Carvalho, M.D.S. The Use of Polyurethane Composites with Sensing Polymers as New Coating Materials for Surface AcousticWave-Based Chemical Sensors—Part I: Analysis of the Coating Results, Sensing Responses and Adhesion of the Coating Layers of Polyurethane–Polybutylmethacrylate Composites. *Coatings* **2023**, *13*, 1911. [CrossRef]